2015

Propagation Failure in Discrete Inhomogeneous Medium Using a Caricature of the Cubic

Elizabeth Lydon
University of Central Florida

PROPAGATION FAILURE IN DISCRETE INHOMOGENEOUS MEDIA USING A CARICATURE OF THE CUBIC

by

ELIZABETH LYDON
B.A. Rollins College, 2012

A thesis submitted in partial fulfilment of the requirements
for the degree of Master of Science
in the Department of Mathematics
in the College of Sciences
at the University of Central Florida
Orlando, Florida

Summer Term
2015

Major Professor: Brian E. Moore

ABSTRACT

Spatially discrete Nagumo equations have widespread physical applications, including modeling electrical impulses traveling through a demyelinated axon, an environment typical in multiple sclerosis. We construct steady-state, single front solutions by employing a piecewise linear reaction term. Using a combination of Jacobi-Operator theory and the Sherman-Morrison formula we derive exact solutions in the cases of homogeneous and inhomogeneous diffusion. Solutions exist only under certain conditions outlined in their construction. The range of parameter values that satisfy these conditions constitutes the interval of propagation failure, determining under what circumstances a front becomes pinned in the media. Our exact solutions represent a very specific solution to the spatially discrete Nagumo equation. For example, we only consider inhomogeneous media with one defect present. We created an original script in MATLAB which algorithmically solves more general cases of the equation, including the case for multiple defects. The algorithmic solutions are then compared to known exact solutions to determine their validity.

TABLE OF CONTENTS

LIST OF FIGURES

LIST OF TABLES

CHAPTER 1: INTRODUCTION

1.1 Overview

A model for electrical impulses traveling through the nervous system was introduced by Hodgkin and Huxley. This model is continuous and involves a complex functional which makes it difficult to solve the system for exact solutions. The Nagumo equation,

$$\phi_t = \phi_{xx} - f(\phi; a) \tag{1.1}$$

is a simplification of the Hodgkin-Huxley model. Typically a cubic nonlinearity,

$$f(\phi; a) = \phi(\phi - 1)(a - \phi), \tag{1.2}$$

where $a \in (0, 1)$ is the detuning parameter, is used in the Nagumo equation to approximate the functional in Hodgkin and Huxley's model [9]. The Nagumo equation is also referred to as the Allen-Cahn equation after the authors who used the model to study crystal growth [2]. We study the spatially discrete Nagumo equation,

$$\dot{\phi}_k(t) = L[\phi_k(t)] - f(\phi_k(t); a) \tag{1.3}$$

where

$$L\phi_k(t) = \alpha_k[\phi_{k+1}(t) - \phi_k(t)] + \alpha_{k-1}[\phi_{k-1}(t) - \phi_k(t)].$$

The Nagumo equation has been used to model calcium waves [11], electrical activity in cardiac tissue [8], and fronts moving through myelinated axons in the nervous system [5], [7]. We are interested in the latter case. Specifically, we want to understand what happens to a front when it

moves through an axon damaged by demyelination, a symptom of multiple sclerosis.

Multiple sclerosis is a disease affecting the nervous system. It causes the deterioration of the myelin sheath, the insulting outer shell of a nerve axon which speeds up the conduction of the action potential. Damage to the myelin sheath is called demyelination. Demyelination can cause a nerve impulse to slow down or stop, causing many who suffer from multiple sclerosis to experience loss of motor skills. In our model, the diffusion coefficients α_k represent the degree of demyelination at node k. If all of the diffusion coefficients are equal, $\alpha_k = \alpha \, \forall k$, we refer to this as homogeneous diffusion. This means that the myelin sheath is uniform throughout the axon. If the myelin sheath is damaged at any point, this means $\exists k \in \mathbb{Z}$ such that $\alpha_k \neq \alpha$, and we refer to these variances in the uniform media as "defects". If defects are present then diffusion is inhomogeneous. By considering (1.3) when defects are present, we are gathering insight into how fronts propagate in a body affected by multiple sclerosis.

Another component of a nerve axon are the nodes of Ranvier. Myelin sheath covers the entire axon except at periodic breaks in the structure. These breaks are the nodes of Ranvier. At these nodes, an action potential forces ionized sodium and potassium to flow in and out of the nerve. This reaction, occurring at the nodes of Ranvier, is what transmits the signal to the next part of the axon, and is described by the reaction term f. Each k in 1.3 represents a node of Ranvier, and ϕ_k is the voltage at node k.

The action potential described by f involves detuning parameter a, which controls the speed and the direction of the front. When diffusion is homogeneous, for every value of α there exist corresponding values of a for which a front becomes pinned in the axon. When diffusion is inhomogeneous and defects are present, they affect where the front becomes pinned as well as the interval of propagation failure.

Definition 1: The *interval of propagation failure* for a front is the range of values of detuning parameter a for which stationary fronts exist. We define the interval of propagation failure by placing conditions on α and a that all stationary front solutions must satisfy.

The study of propagation failure is vast. Propagation failure occurs when a front becomes pinned at any point in the medium. Several authors examine propagation failure in homogeneous media of a continuous Nagumo equation [1, 8, 11]. We are interested in studying the discrete Nagumo equation, because the nerve environment is more discrete than continuous in nature due to the placement of the nodes of Ranvier making a discrete equation a more accurate model than the continuous equation. We also believe that studying the discrete Nagumo equation can yield important insights lost in a continuous model. The discrete and continuous Nagumo models are compared in [6]. Studies of "wave block" of calcium waves in spatially inhomogeneous media have been done in [1, 11]. Propagation failure on a two-dimensional lattice with homogeneous diffusion and a discontinuous nonlinearity has been explored in [3].

The nonlinearity f plays a crucial role in determining the interval of propagation failure because of the detuning parameter a. Different nonlinearities change the interval for which the speed of the front is zero. Commonly, authors employ the caricatures of the cubic function suggested by McKean [9]

$$f(\phi; a) = \phi - h(\phi - a) \tag{1.4}$$

where H is the Heaviside function:

$$h(\phi) = \begin{cases} 1 & \phi > 0 \\ [0,1] & \phi = 0 \\ 0 & \phi < 0 \end{cases}$$

or

$$f(\phi;a) = \begin{cases} \phi, & \phi \leq a/2 \\ a-\phi, & a/2 < \phi < (a+1)/2 \\ \phi - 1, & \phi \geq (a+1)/2 \end{cases} \tag{1.5}$$

where $a \in (0,1)$. The differences in (1.4) and (1.5) are seen in the Figure 1.1.

The following sources all use McKean's discontinuous caricature (1.4) [1, 4, 6, 7]. The discontinuous nonlinearity is easier to work with and allows for solutions to traveling fronts. However the discontinuity makes results for the interval of propagation failure artificial. The spatially discrete Nagumo equation with homogeneous diffusion has been solved by [5] using the continuous piecewise linear nonlinearity prescribed by McKean (1.5). Either choice in f is an approximation of the original functional suggested by Hodgkin and Huxley, just as the cubic (1.2) is an approximation of that functional. Our paper uses the same piecewise continuous nonlinearity (1.5) as [5], but we employ the techniques from [7] to solve for single-front, steady-state solutions to (1.3) with inhomogeneous diffusion. We examine the interval of propagation failure for these solutions.

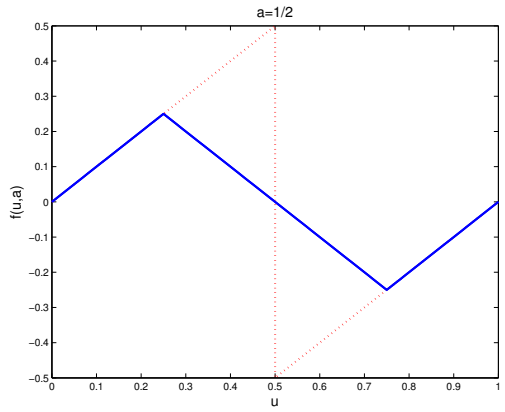

Figure 1.1: Discontinuous nonlinearity (1.4) in red, continuous sawtooth nonlinearity (1.5) in blue.

To explore the role of the detuning parameter further, we examine the Nagumo equation (1.3) when

there is no diffusion, or $L[\phi_k(t)] = 0$. Thus we are considering the behavior of a single node as it changes over time with the equation

$$\dot{\phi}_k(t) = \frac{d\phi}{dt} = -f(\phi; a). \tag{1.6}$$

The general solutions of (1.6) are as follows:

$$\phi = \begin{cases} c_1 e^{-t} & \phi \leq a/2 \\ a + c_2 e^{t} & a/2 < \phi < (a+1)/2 \\ 1 + c_3 e^{-t} & (a+1)/2 \leq \phi \end{cases} \tag{1.7}$$

where $|c_1|, |c_2|, |c_3| \in (0, 1)$.

Using 1.6, we graphϕ vs. $\frac{d\phi}{dt}$ as in Figure 1.2 which shows us that $\frac{d\phi}{dt} < 0$ when $\phi < a/2$, thus we require constant $c_1 > 0$ in (1.7) to ensure a negative slope in the solution ϕ. This means that if the voltage of ϕ is initially less that $a/2$, such solutions tend to zero as $t \to \infty$. Similarly, the derivative $\frac{d\phi}{dt} > 0$ if $\phi > (a+1)/2$, so we need $c_3 < 0$ in (1.7) for the solution ϕ to have a positive slope. If the voltage of ϕ is initially greater than $(a+1)/2$, then $\phi \to 1$ as $t \to \infty$. If $c_2 < 0$ and we are in the second case of (1.7), then $\phi \leq a \, \forall t > 0$, and as $t \to \infty$, $\phi \to 0$. A solution demonstrating this behavior is depicted in the left panel of Figure 1.3. If $c_2 > 0$ and we are in the second case of (1.7) then $\phi \geq a \, \forall t > 0$ and as $t \to \infty$, $\phi \to 1$. A solution depicted in the right panel of Figure 1.3 is an example of this.

Figures 1.2 and 1.3 also tell us that a is an unstable equilibrium point. If $\phi < a$, the individual node will turn off as time elapses and the voltage will go to zero. If $\phi > a$, the individual node will turn on as $t \to \infty$. The closer a is to zero, the more likely it is that $\phi \to 1$ as time goes on. The closer a is to 1, it is more probable that $\phi \to 0$.

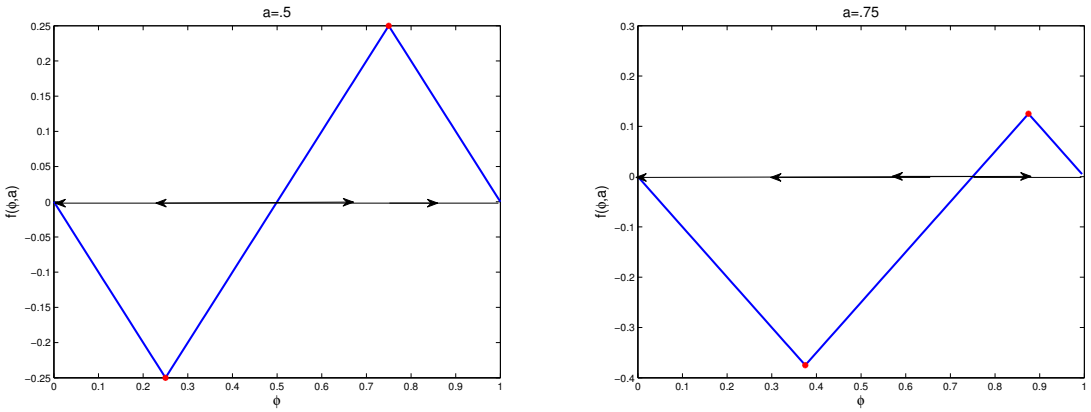

Figure 1.2: Plotting ϕ vs. $\frac{d\phi}{dt}$.

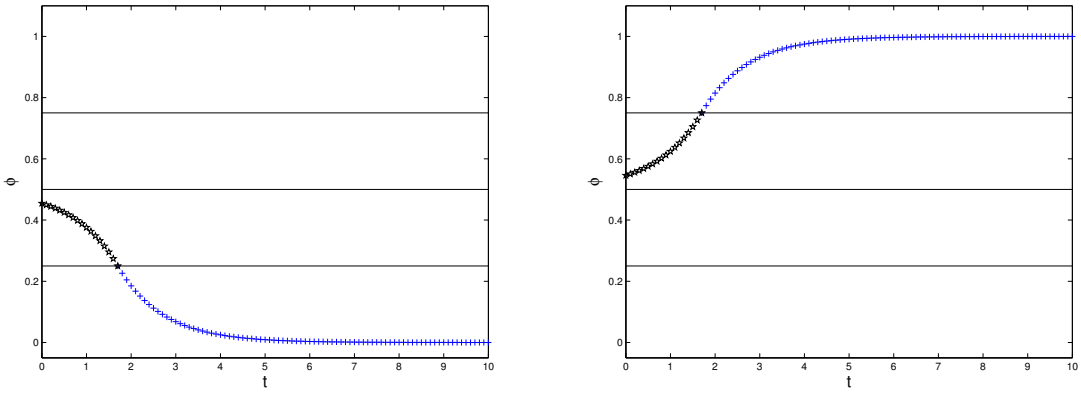

Figure 1.3: Candidate solutions to (1.6). The black dotted lines, from bottom to top, represent $y = a/2$, $y = a$, and $y = (a + 1)/2$, respectively.

When we consider the Nagumo equation with diffusion ($L[\phi_k(t)] \neq 0$), the voltage of a single node ϕ_k interacts with its surrounding nodes. When $a > 1/2$ this yields a right moving front (see right panel of Figure 1.4). This means the signal is turning off the voltage at each node in the nerve axon, and $\phi_k \to 0$ as $t \to \infty$. When $a < 1/2$, this produces a left moving front (see left panel of Figure 1.4), or the impulse is turning the voltage at each node on. This means all of the nodes in the axon are turned on, and $\phi_k \to 1$ as $t \to \infty$. When $a = 1/2$ as in the left panel of Figure 1.2,

ϕ_k is pulled equally towards 0 and towards 1, yielding a stationary front.

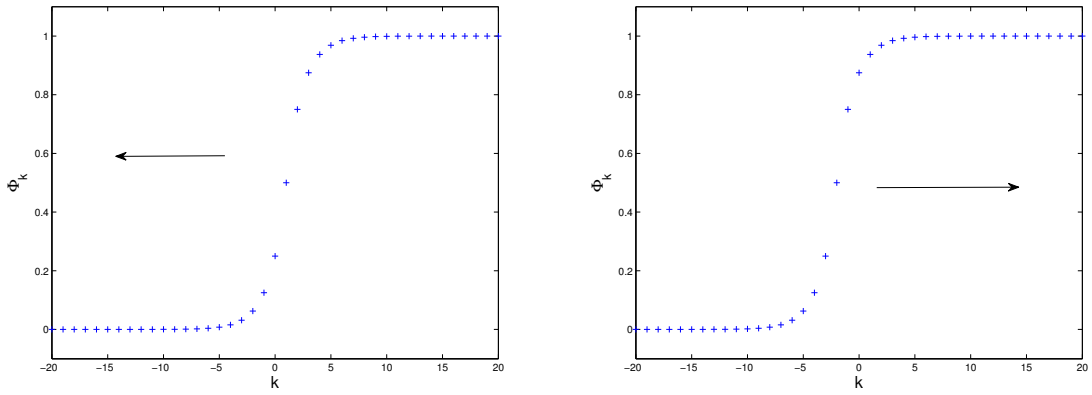

Figure 1.4: Plots of traveling front solutions. In left panel $a < 1/2$, in the right panel $a > 1/2$.

The structure of f and a's role in the reaction term determines the interval of propagation failure. There are choices of nonlinearity for which no stationary fronts exist [5]. As [8] asserts, finding the interval of propagation failure for solutions to (1.3) is equivalent to finding the conditions for which stationary fronts exist. These conditions are stated in the next section 1.2, and we use them to construct solutions for homogeneous and inhomogeneous media in Chapters 2 and 3, with the end of Chapter 3 devoted to comparing the intervals of propagation failure of the two cases. The solutions constructed in this paper for (1.3) with (1.5) in the case of inhomogeneous media are original results, and we have presented a new way of solving the homogeneous case. We explore the case of inhomogeneous diffusion with just one defect present in Chapter 3. Solving for exact solutions with multiple defects present is tedious, thus we've created an original script in MATLAB capable of algorithmically solving (1.3) with as many defects as we choose, with different choices of nonlinearity f, and any position of the wave. Chapter 4 compares our exact solutions found in Chapters 2 and 3 with solutions found algorithmically using our code. Results are summarized and ideas for future work are discussed in Chapter 5.

1.2 Preliminaries for our problem

We seek steady-state, single front solutions of

$$\dot{\phi}_k(t) = L\phi_k(t) - f(\phi_k(t); a) \tag{1.8}$$

where $\phi_k(t)$ maps $\mathbb{R}^+ \cup \{0\} \to \mathbb{R}$, $k \in \mathbb{Z}$ indicates an element of a one-dimensional lattice, $\dot{\phi} = \frac{d\phi}{dt}$,

$$L\phi_k(t) = \alpha_k[\phi_{k+1}(t) - \phi_k(t)] + \alpha_{k-1}[\phi_{k-1}(t) - \phi_k(t)],$$

and using $\alpha_k \in \mathbb{R}^+$ and $p, q \in \{0\} \cup \mathbb{Z}^+$, the inhomogeneous medium is defined by

$$\alpha_k = \alpha \quad \text{for} \quad k < -p \text{ or } k > q \qquad \text{and} \qquad \alpha_k \neq \alpha \quad \text{for} \quad -p \leq k \leq q$$

$f : \mathbb{R} \to \mathbb{R}$ is the derivative of a double-well potential. To derive exact solutions we employ reaction term (1.5), and set boundary conditions

$$\lim_{k \to -\infty} \phi_k = 0 \qquad \text{and} \qquad \lim_{\mathrm{k} \to \infty} \phi_{\mathrm{k}} = 1. \tag{1.9}$$

To solve for standing front solutions of (1.3) we set $\dot{\phi}_j(t) = 0$, or

$$\alpha_k(\phi_{k+1} - \phi_k) + \alpha_{k-1}(\phi_{k-1} - \phi_k) - f(\phi_k; a) = 0 \tag{1.10}$$

to get an equation independent of time t. In order to solve (1.10) we make some assumptions that allow us to rewrite nonlinearity f in a linear form. Once we do this, we can solve (1.10) as a difference equation. These assumptions also give us a way to determine where the stationary front

is in the medium. This is critical when considering inhomogeneous diffusion because the interval of propagation failure varies depending on where the front is. Note that

$$f(\phi_k; a) = \phi_k \begin{cases} 1 & \phi_k \leq a/2 \\ -1 & a/2 < \phi_k < (a+1)/2 \\ 1 & (a+1)/2 \leq \phi_k \end{cases} + \begin{cases} 0 & \phi_k \leq a/2 \\ a & a/2 < \phi_k < (a+1)/2 \\ -1 & (a+1)/2 \leq \phi_k \end{cases} \tag{1.11}$$

Define $\varphi(x, \eta_0) = \phi_k$ to be a continuous function that interpolates ϕ_k at any $x \in \mathbb{R}$, and assume that φ only crosses $a/2$ and $(a+1)/2$ once at

$$a/2 = \varphi(\eta_0; \eta_0), \qquad (a+1)/2 = \varphi(\eta_1; \eta_0)$$

In other words, η_0 is the spatial location at which φ takes the value $a/2$, and η_1 is the spatial location at which φ takes the value $(a+1)/2$. Thus we can say that $\varphi(x, \eta_0) < a/2$ for $x < \eta_0$ and similarly that $a/2 < \varphi(x, \eta_0) < (a+1)/2$ for $\eta_0 < x < \eta_1$ and $\varphi(x, \eta_0) > (a+1)/2$ for $x > \eta_1$. Thus

$$\phi_k \leq a/2 \quad \text{for} \quad \mathrm{k} \leq \eta_0 \tag{1.12}$$

$$a/2 < \phi_k < (a+1)/2 \quad \text{for} \quad \eta_0 < \mathrm{k} < \eta_1 \tag{1.13}$$

$$(a+1)/2 \leq \phi_k \quad \text{for} \quad \mathrm{k} \geq \eta_1. \tag{1.14}$$

Let n equal the number of $\phi_k \in [a/2, (a+1)/2]$. We define $k^* = \lfloor \eta_0 \rfloor$ and $k^* + n + 1 = \lceil \eta_1 \rceil$.

Remark: For the purpose of this thesis, assume one point lies between η_0 and η_1. That is, $n = 1$.

Then

$$\phi_k \leq a/2 \quad \text{for} \quad \mathrm{k} \leq \mathrm{k}^* \tag{1.15}$$

$$a/2 < \phi_k < (a+1)/2 \quad \text{for} \quad \mathrm{k} = \mathrm{k}^* + 1 \tag{1.16}$$

$$(a+1)/2 \leq \phi_k \quad \text{for} \quad \mathrm{k} \geq \mathrm{k}^* + 2. \tag{1.17}$$

and ϕ_{k^*+1} is the only node lying in the interval $[a/2, (a+1)/2]$. Now we can write f as

$$f(\phi_k; a) = \phi_k \begin{cases} 1 & k \leq k^* \\ -1 & k = k^* + 1 \\ 1 & k \geq k^* + 2 \end{cases} + \begin{cases} 0 & k \leq k^* \\ a & k = k^* + 1 \\ -1 & k \geq k^* + 2 \end{cases} \tag{1.18}$$

or as

$$f(\phi_k, a) = v_k \phi_k - w_k \tag{1.19}$$

where

$$v_k = \begin{cases} 1, & k \leq k^* \\ -1, & k = k^* + 1 \\ 1, & k \geq k^* + 2 \end{cases} \quad \text{and} \quad w_k = \begin{cases} 0, & k \leq k^* \\ -a, & k = k^* + 1 \\ 1, & k \geq k^* + 2 \end{cases} . \tag{1.20}$$

Now f is linear in k and we can write (1.10) as

$$-\alpha_k \phi_{k+1} + (v_k + \alpha_k + \alpha_{k-1})\phi_k - \alpha_{k-1}\phi_{k-1} = w_k \qquad \forall k \tag{1.21}$$

which is a second order linear difference equation.

In past works [7, 10], Jacobi operator theory has been used to solve equations like (1.21) because the method is useful when considering inhomogeneous media, or varying α_k. Jacobi operator theory dictates that the coefficients of ϕ_k depend solely on the position k in the lattice [12]. Un-

fortunately, the coefficient v_k in (1.21) depends on k and k^*, violating the definition of a Jacobi operator. Note that, (1.21) is the same as

$$-\alpha_k\phi_{k+1} + (1 + \alpha_k + \alpha_{k-1})\phi_k - \alpha_{k-1}\phi_{k-1} = w_k \tag{1.22}$$

except when $k = k^* + 1$ when (1.21) is

$$-\alpha_{k^*+1}\phi_{k^*+2} + (-1 - \alpha_{k^*+1} + \alpha_{k^*})\phi_{k^*+1} - \alpha_{k^*}\phi_k^* = -a. \tag{1.23}$$

We can also view (1.22) as an infinite tridiagonal system of equations where

$$M_{ij} = \begin{cases} \alpha_i & i = j + 1 \\ (1 + \alpha_i + \alpha_{i-1}) & i = j \\ \alpha_{i-1} & i = j - 1 \\ 0 & \text{otherwise,} \end{cases}$$

and

$$\phi = [...\phi_k \ \phi_{k+1} \ \phi_{k+2}...]^T,$$

and

$$w = [...w_k \ w_{k+1} \ w_{k+2}...]^T$$

so that (1.22) is also $\mathbf{M}\phi = \mathbf{w}$, where $\mathbf{M}$ is a Jacobi operator, and the system can be solved using the method outlined in [7].

We can solve (1.21) using the Sherman-Morrison formula which solves systems of equations that are perturbations of systems with already known solutions. Note, (1.21) can be represented $\mathbf{T}\hat{\phi} = \mathbf{w}$ with $\mathbf{T} = \mathbf{M} + \mathbf{\Delta T}$ where $\mathbf{\Delta T}$ represents the change/perturbation when $k = k^* + 1$. We already know how to solve $\mathbf{M}\phi = \mathbf{w}$ using Jacobi operator theory, which we do in Chapter 2. In Chapter

3 we outline how to use the solutions for $\mathbf{M}\phi = \mathbf{w}$ from Chapter 2 with the Sherman-Morrison formula to solve our original problem $\mathbf{T}\hat{\phi} = \mathbf{w}$.

CHAPTER 2: SOLVING $\mathrm{M}\phi = \mathbf{w}$

To arrive at the solution for (1.21) we must first derive the solutions for (1.22),

$$-\alpha_k\phi_{k+1} + (1 + \alpha_k + \alpha_{k-1})\phi_k - \alpha_{k-1}\phi_{k-1} = w_k \quad \forall k \in \mathbb{Z}. \tag{2.1}$$

We consider solutions to this equation when diffusion is both homogeneous and inhomogeneous following the method outlined in [7].

2.1 Homogeneous Diffusion

To consider (1.22) with homogeneous diffusion we set $\alpha_k = \alpha \ \forall k$. Thus (1.22) becomes

$$-\alpha\phi_{k+1} + (2\alpha + 1)\phi_k - \alpha\phi_{k-1} = w_k \qquad \forall k \in \mathbb{Z} \tag{2.2}$$

a second-order linear difference equation. The general solution to (2.2) will consist of two fundamental solutions and one particular solution. To find the fundamental solutions, we start by setting the right hand side of (2.2) equal to zero which yields

$$-\alpha\phi_{k+1} + (2\alpha + 1)\phi_k - \alpha\phi_{k-1} = 0 \qquad \forall k \in \mathbb{Z} \tag{2.3}$$

or alternatively,

$$\phi_{k+1} + \phi_{k-1} = 2\mu\phi_k \tag{2.4}$$

where μ is defined

$$\mu = \frac{2\alpha + 1}{2\alpha}. \tag{2.5}$$

The solutions of (2.3) will be of the form

$$\phi_k = \phi_{k_0}\rho(k-k_0) + \phi_{k_0+1}\sigma(k-k_0) \tag{2.6}$$

where k_0 is any initial starting point, and $\rho(k-k_0)$ and $\sigma(k-k_0)$ are two linearly independent fundamental solutions. Without loss in generality, we keep $k_0 = k^*$ throughout this paper. To ensure $\rho(k-k^*)$ and $\sigma(k-k^*)$ are linearly independent, we choose the following set of linearly independent initial conditions

$$\rho(0) = 1, \quad \rho(1) = 0, \quad \sigma(0) = 0, \quad \sigma(1) = 1. \tag{2.7}$$

To find expressions for $\rho(k-k^*)$ and $\sigma(k-k^*)$ we set $\phi_k = \lambda^k$ and plug this into (2.3). This leads us to the auxiliary equation $\lambda^2 - 2\mu\lambda + 1 = 0$. Solving for λ we see $\lambda_\pm = \mu \pm \sqrt{\mu^2-1} = 1 + \frac{1}{2\alpha} \pm \frac{\sqrt{4\alpha+1}}{2\alpha}$. Note that $\lambda_+\lambda_- = 1$. If we take $\lambda = \lambda_+$ then the two solutions are λ and λ^{-1} with $\lambda^{-1} < 1 < \lambda$.

Using the initial conditions (2.7), we arrive at the expressions for the fundamental solutions:

$$\rho(k-k^*) = \frac{\lambda^{1+k^*-k} - \lambda^{k-1-k^*}}{\lambda - \lambda^{-1}} \qquad \text{and} \qquad \sigma(\mathrm{k}-\mathrm{k}^*) = \frac{\lambda^{\mathrm{k}-\mathrm{k}^*} - \lambda^{\mathrm{k}^*-\mathrm{k}}}{\lambda - \lambda^{-1}}. \tag{2.8}$$

According to [12], the general solution to (2.2) is

$$\phi_k = \phi_{k^*}\rho(k-k^*) + \phi_{k^*+1}\sigma(k-k^*) + \begin{cases} \sum_{j=k^*+1}^{k} \frac{-1}{\alpha_j} w_j \sigma(k-j) & k > k^* \\ 0 & k = k^* \\ \sum_{j=k^*+1}^{k} \frac{1}{\alpha_j} w_j \sigma(k-j) & k < k^* \end{cases} \tag{2.9}$$

where w_j is as defined in (1.20). It can be verified that

$$\phi_k = \begin{cases} \sum_{j=k^*+1}^{k} \frac{-1}{\alpha_j} w_j \sigma(k-j) & k > k^* \\ 0 & k = k^* \\ \sum_{j=k^*+1}^{k} \frac{1}{\alpha_j} w_j \sigma(k-j) & k < k^* \end{cases}$$

is a particular solution to (2.2). Because $w_j = 0$ for $j \leq k^*$ we can simplify (2.9) to

$$\phi_k = \phi_{k^*}\rho(k-k^*) + \phi_{k^*+1}\sigma(k-k^*) + \begin{cases} \sum_{j=k^*+1}^{k} \frac{-1}{\alpha_j} w_j \sigma(k-j) & k > k^* \\ 0 & k \leq k^*. \end{cases} \tag{2.10}$$

We still need to determine the coefficients ϕ_{k^*} and ϕ_{k^*+1}. Because we are considering homogeneous diffusion, it is without loss in generality that we choose $k^* = 0$ since the medium is translationally invariant. We use the boundary conditions (1.9) to set up a system of equations to solve for these coefficients.

As $k \to -\infty$, $\phi_k \to 0$, and

$$\phi_k = \phi_0\rho(k) + \phi_1\sigma(k) = 0.$$

By factoring and separating the λ^k terms from the λ^{-k} terms we get

$$\phi_k = \frac{\lambda^{-k}}{\lambda - \lambda^{-1}} \left[\lambda\phi_0 - \phi_1\right] - \frac{\lambda^k}{\lambda - \lambda^{-1}} \left[\lambda^{-1}\phi_0 - \phi_1\right],$$

in which the first term tends to infinity as $k \to -\infty$. Thus we must require that

$$\lambda\phi_0 - \phi_1 = 0. \tag{2.11}$$

As $k \to \infty$

$$\phi_k = \phi_0 \rho(k) + \phi_1 \sigma(k) - \frac{1}{\alpha} \sum_{j=1}^{k} w_j \sigma(k-j).$$

As before, factor and separate the λ^k terms from the λ^{-k} terms to get

$$\phi_k = \frac{\lambda^{-k}}{\lambda - \lambda^{-1}} \left[\lambda\phi_0 - \phi_1 - \frac{a\lambda}{\alpha} + \frac{1}{\alpha} \sum_{j=2}^{k} \lambda^j \right] - \frac{\lambda^k}{\lambda - \lambda^{-1}} \left[\lambda^{-1}\phi_0 - \phi_1 - \frac{a\lambda^{-1}}{\alpha} + \frac{1}{\alpha} \sum_{j=2}^{k} \lambda^{-j} \right].$$

Recall the formula for the sum of a geometric series is $\sum_{j=2}^{k} \lambda^j = \frac{\lambda^k - \lambda}{1-\lambda^{-1}}$ and $\sum_{j=2}^{k} \lambda^{-j} = \frac{\lambda^{-k} - \lambda^{-1}}{1-\lambda}$. The second term grows infinitely large as $k \to \infty$ and we require

$$0 = \lim_{k\to\infty} \left[\lambda^{-1}\phi_0 - \phi_1 - \frac{a\lambda^{-1}}{\alpha} + \frac{1}{\alpha} \sum_{j=2}^{k} \lambda^{-j} \right] = \lim_{k\to\infty} \left[\lambda^{-1}\phi_0 - \phi_1 - \frac{a\lambda^{-1}}{\alpha} + \frac{1}{\alpha} \left(\frac{\lambda^{-k} - \lambda^{-1}}{1-\lambda} \right) \right]$$

Thus we need

$$\lambda^{-1}\phi_0 - \phi_1 - \frac{a\lambda^{-1}}{\alpha} + \frac{\lambda^{-1}}{\alpha(\lambda - 1)} = 0. \tag{2.12}$$

We use (2.11) and (2.12) to solve for ϕ_0 and ϕ_1, which yields

$$\phi_0 = \frac{a(\lambda^{-1} - 1) + \lambda^{-1}}{\lambda + 1}, \qquad \text{and} \qquad \phi_1 = \frac{a(1-\lambda) + 1}{\lambda + 1}. \tag{2.13}$$

Plugging ϕ_0 and ϕ_1 into the general solution reduces (2.9) to

$$\phi_k = \begin{cases} \lambda^{1-k}(\phi_1 - 1) + 1 & k > 0 \\ \lambda^k \phi_0 & k \leq k^*. \end{cases} \tag{2.14}$$

We will revisit these solutions in section 3.1.

2.2 Inhomogeneous Diffusion

We consider

$$-\alpha_k\phi_{k+1} + (1 + \alpha_k + \alpha_{k-1})\phi_k - \alpha_{k-1}\phi_{k-1} = w_k \tag{2.15}$$

when $p = q = 0$, i.e. in the case of one defect at α_0. Because the medium is inhomogeneous and no longer translationally invariant, the fundamental solutions will differ depending on the position of k^* relative to the defect at $k = 0$. There are three cases to consider: $k^* < 0$, $k^* = 0$, and $k^* > 0$. To construct the fundamental solutions we follow Lemma 3.3 outlined in [7]. In fact, our fundamental solutions will be the same as the fundamental solutions derived in Section 3.1 of [7] because our homogeneous equations are the same. We have the same initial conditions on starting point k^*

$$\tilde{\rho}(k^*, k^*) = 1, \quad \tilde{\rho}(k^* + 1, k^*) = 0, \quad \tilde{\sigma}(k^*, k^*) = 0, \quad \tilde{\sigma}(k^* + 1, k^*) = 1. \tag{2.16}$$

When $k^* = 0$, the fundamental solutions are

$$\tilde{\rho}(k, 0) = \begin{cases} \tau\rho(k) & k > 0 \\ \nu\rho(k+1) - \rho(k+2) & k \leq 0 \end{cases} \quad \tilde{\sigma}(k, 0) = \begin{cases} \nu\sigma(k-1) - \sigma(k-2) & k > 0 \\ \tau\sigma(k) & k \leq 0 \end{cases} \tag{2.17}$$

where we define $\tau = \frac{\alpha_0}{\alpha}$ and $\nu = \frac{1+\alpha+\alpha_0}{\alpha}$. When $k^* < 0$ or $k^* > 0$ the solutions are defined

$$\tilde{\rho}(k, k^*) = \begin{cases} \rho(k-1)\theta(1, k^*) + \sigma(k-1)\theta(2, k^*) & k \geq 0, k^* < 0 \\ \rho(k - k^*) & k \leq 0, k^* < 0, \text{ or } k \geq 0, k^* > 0 \\ \rho(k+1)\theta(-1, k^*) + \sigma(k+1)\theta(0, k^*) & k \leq 0, k^* > 0 \end{cases} \tag{2.18}$$

and

$$\tilde{\sigma}(k,k^*) = \begin{cases} \rho(k-1)\zeta(1,k^*) + \sigma(k-1)\zeta(2,k^*) & k \geq 0, k^* < 0 \\ \sigma(k-k^*) & k \leq 0, k^* < 0, \text{ or } k \geq 0, k^* > 0 \\ \rho(k+1)\zeta(-1,k^*) + \sigma(k+1)\zeta(0,k^*) & k \leq 0, k^* > 0 \end{cases} \tag{2.19}$$

where

$$\begin{aligned} \theta(1,k^*) &= \frac{1}{\tau}(\nu\rho(-k^*) - \rho(-1-k^*)) \\ \theta(2,k^*) &= \frac{1}{\tau}((\nu^2-\tau^2)\rho(-k^*) - \nu\rho(-1-k^*)) \\ \zeta(1,k^*) &= \frac{1}{\tau}(\nu\sigma(-k^*) - \sigma(-1-k^*)) \\ \zeta(2,k^*) &= \frac{1}{\tau}((\nu^2-\tau^2)\sigma(-k^*) - \nu\sigma(-1-k^*)) \\ \theta(0,k^*) &= \frac{1}{\tau}(\nu\rho(1-k^*) - \rho(2-k^*)) \\ \theta(-1,k^*) &= \frac{1}{\tau}((\nu^2-\tau^2)\rho(1-k^*) - \nu\rho(2-k^*)) \\ \zeta(0,k^*) &= \frac{1}{\tau}(\nu\sigma(1-k^*) - \sigma(2-k^*)) \\ \zeta(-1,k^*) &= \frac{1}{\tau}((\nu^2-\sigma^2)\sigma(1-k^*) - \nu\sigma(2-k^*)). \end{aligned}$$

The general solution $\forall k^* \in \mathbb{Z}$ is

$$\phi_k = \phi_{k^*}\tilde{\rho}(k,k^*) + \phi_{k^*+1}\tilde{\sigma}(k,k^*) + \begin{cases} \sum_{j=k^*+1}^{k} \frac{-1}{\alpha_j} w_j \tilde{\sigma}(k,j) & k > k^* \\ 0 & k \leq k^*. \end{cases} \tag{2.20}$$

We explicitly solve two difference cases: $k^* = -1$ and $k^* = 0$. From our definition of k^* in (1.15)-(1.17), when $k^* = -1$ the interface of the front lies at the defect, α_0. When $k^* = 0$, the interface lies after the defect at $k = 1$. The case when the front is at the defect ($k^* = -1$) is of significant

importance because we want to know if $\exists a \in (0,1)$ that yield traveling fronts when $\alpha_0 = \alpha$, but yield stationary fronts when $\alpha_0 < \alpha$. When we examine the interval of propagation failure for fronts after the defect ($k^* = 0$), we want to see if $\forall a \in (0,1)$ that yield traveling fronts when $\alpha_0 = \alpha$ also yield traveling fronts when $\alpha_0 < \alpha$. We want to compare these results to Theorem 3.2 in [7].

2.2.1 Fronts at the defect

The general form of (2.20) when $k^* = -1$ is

$$\phi_k = \phi_{-1}\tilde{\rho}(k,-1) + \phi_0\tilde{\sigma}(k,-1) + \begin{cases} \sum_{j=0}^{k} \frac{-1}{\alpha_j}\tilde{\sigma}(k,j) & k > -1 \\ 0 & k \leq -1 \end{cases} \tag{2.21}$$

with the fundamental solutions found in (2.17)-(2.19). Once more we employ boundary conditions (1.9) to solve for the coefficients ϕ_{-1} and ϕ_0. As $k \to -\infty$

$$\phi_k = \frac{\lambda^{-k}}{\lambda - \lambda^{-1}}(\phi_{-1} - \lambda^{-1}\phi_0) - \frac{\lambda^{k}}{\lambda - \lambda^{-1}}(\phi_{-1} - \lambda\phi_0) = 0.$$

To prevent the first term from diverging we set

$$\phi_{-1} - \lambda^{-1}\phi_0 = 0. \tag{2.22}$$

As $k \to \infty$

$$\begin{aligned}\phi_k =& \frac{\lambda^{-k}}{\tau(\lambda - \lambda^{-1})}((\nu\lambda - \lambda^2)\phi_{-1} + (\nu\lambda^2 - \lambda(\nu^2 - \tau^2))\phi_0 + \frac{\tau a}{\alpha_0}(\lambda^2 - \nu\lambda) + \frac{\tau}{\alpha}\sum_{j=1}^{k}\lambda^j) \\ &- \frac{\lambda^{k}}{\tau(\lambda - \lambda^{-1})}((\nu\lambda^{-1} - \lambda^{-2})\phi_{-1} + (\nu\lambda^{-2} - \lambda^{-1}(\nu^2 - \tau^2))\phi_0 + \frac{\tau a}{\alpha_0}(\lambda^{-2} - \nu\lambda^{-1}) + \frac{\tau}{\alpha}\sum_{j=1}^{k}\lambda^{-j}).\end{aligned}$$

Recall that $\sum_{j=1}^{k} \lambda^j = \frac{\lambda^k - 1}{1-\lambda^{-1}}$ and $\sum_{j=1}^{k} \lambda^{-j} = \frac{\lambda^{-k}-1}{1-\lambda}$. To satisfy the boundary conditions we require

$$\lim_{k\to\infty} \left[(\nu\lambda^{-1} - \lambda^{-2})\phi_{-1} + (\nu\lambda^{-2} - \lambda^{-1}(\nu^2 - \tau^2))\phi_0 + \frac{\tau a}{\alpha_0}(\lambda^{-2} - \nu\lambda^{-1}) + \frac{\tau}{\alpha}\sum_{j=1}^{k} \lambda^{-j} \right] \tag{2.23}$$

$$= \lim_{k\to\infty} \left[(\nu\lambda^{-1} - \lambda^{-2})\phi_{-1} + (\nu\lambda^{-2} - \lambda^{-1}(\nu^2 - \tau^2))\phi_0 + \frac{\tau a}{\alpha_0}(\lambda^{-2} - \nu\lambda^{-1}) + \frac{\tau(\lambda^{-k} - 1)}{\alpha(1-\lambda)} \right] \tag{2.24}$$

$$= (\nu\lambda^{-1} - \lambda^{-2})\phi_{-1} + (\nu\lambda^{-2} - \lambda^{-1}(\nu^2 - \tau^2))\phi_0 + \frac{\tau a}{\alpha_0}(\lambda^{-2} - \nu\lambda^{-1}) + \frac{\tau}{\alpha}\frac{1}{\lambda - 1} \tag{2.25}$$

$$= (\nu - \lambda^{-1})\phi_{-1} + (\nu\lambda^{-1} - (\nu^2 - \tau^2))\phi_0 + \frac{\tau a}{\alpha_0}(\lambda^{-1} - \nu) + \frac{\tau\lambda}{\alpha(\lambda - 1)} = 0 \tag{2.26}$$

We solve 2.22 and 2.26 for ϕ_{-1} and ϕ_0 and

$$\phi_{-1} = \frac{(a(\lambda + \tau - 1) - \alpha_0(\lambda - 1))}{\alpha(-\lambda^3 + 2\lambda^2 - 2\lambda^2\tau + 2\lambda\tau - \lambda)} \qquad \phi_0 = \frac{\lambda(a(\lambda + \tau - 1) - \alpha_0(\lambda - 1))}{\alpha(-\lambda^3 + 2\lambda^2 - 2\lambda^2\tau + 2\lambda\tau - \lambda)} \tag{2.27}$$

Substituting these expressions back into the general solution 2.21 we see

$$\phi_k = \begin{cases} 1 + \frac{\lambda^{1-k}\tau}{\lambda + \tau - 1}(\phi_0 - 1) & k > 0 \\ \lambda^{k+1}\phi_{-1} & k \leq 0. \end{cases} \tag{2.28}$$

We will use employ these solutions further in section 3.2.1.

2.2.2 *Fronts after the defect*

Once again, we will use the boundary conditions (1.9) and (2.20) in order to find the coefficients ϕ_0 and ϕ_1 when $k^* = 0$. As $k \to -\infty$ we see

$$\phi_k = \frac{\lambda^{-k}}{\lambda - \lambda^{-1}}\Big(\phi_0(\nu - \lambda^{-1}) - \tau\phi_1\Big) - \frac{\lambda^{k}}{\lambda - \lambda^{-1}}\Big(\phi_0(\nu - \lambda) - \tau\phi_1\Big) \tag{2.29}$$

Note that $\nu = \frac{1+\alpha+\alpha_0}{\alpha} = 2\mu - 1 + \frac{\alpha_0}{\alpha} = \lambda + \lambda^{-1} + \tau - 1$. In order to satisfy our boundary conditions as $k \to -\infty$ we need

$$\phi_0(\nu - \lambda^{-1}) - \tau\phi_1 = 0 \quad \Leftrightarrow \quad \phi_0(\lambda + \tau - 1) - \tau\phi_1 = 0. \tag{2.30}$$

As $k \to \infty$ we have

$$\begin{aligned}\phi_k = &\frac{\lambda^{-k}}{\lambda - \lambda^{-1}}\Big(\lambda\tau\phi_0 - \phi_1(\nu\lambda - \lambda^2) - \frac{a\lambda}{\alpha} + \frac{1}{\alpha}\sum_{j=2}^{k}\lambda^j\Big)\\ &- \frac{\lambda^{k}}{\lambda - \lambda^{-1}}\Big(\lambda^{-1}\tau\phi_0 - \phi_1(\nu\lambda^{-1} - \lambda^{-2}) - \frac{a\lambda^{-1}}{\alpha} + \frac{1}{\alpha}\sum_{j=2}^{k}\lambda^{-j}\Big),\end{aligned}$$

and we require

$$\lim_{k\to\infty}\left[\lambda^{-1}\tau\phi_0 - \phi_1(\nu\lambda^{-1} - \lambda^{-2}) - \frac{a\lambda^{-1}}{\alpha} + \frac{1}{\alpha}\sum_{j=2}^{k}\lambda^{-j}\right] \tag{2.31}$$

$$= \lim_{k\to\infty}\left[\lambda^{-1}\tau\phi_0 - \phi_1(\nu\lambda^{-1} - \lambda^{-2}) - \frac{a\lambda^{-1}}{\alpha} + \frac{\lambda^{-k} - \lambda^{-1}}{\alpha(1-\lambda)}\right] \tag{2.32}$$

$$= \lambda^{-1}\tau\phi_0 - \phi_1(\nu\lambda^{-1} - \lambda^{-2}) - \frac{a\lambda^{-1}}{\alpha} + \frac{\lambda^{-1}}{\alpha(\lambda - 1)} = 0 \tag{2.33}$$

We use (2.30) and (2.33) to solve for ϕ_0 and ϕ_1 and

$$\phi_0 = \frac{\tau(a(\lambda^{-1}-1)+\lambda^{-1})}{\lambda+2\tau-1} \qquad \text{and} \qquad \phi_1 = \frac{(\lambda+\tau-1)(a(\lambda^{-1}-1)+\lambda^{-1})}{\lambda+2\tau-1} \tag{2.34}$$

If we plug (2.34) into (2.20) the simplified version of the general solution is

$$\phi_k = \begin{cases} \lambda^{1-k}(\phi_1-1)+1 & k>0 \\ \lambda^k\phi_0 & k\leq 0. \end{cases} \tag{2.35}$$

These solutions are not the same as those found in section 2.1 because coefficients ϕ_0 and ϕ_1 are different. Again, we revisit this solution in section 3.2.2.

CHAPTER 3: SOLVING $(\mathbf{M} + \mathbf{\Delta T})\phi = \mathbf{w}$

Now that we have found the solutions $\phi = \mathbf{M^{-1}w}$ to $\mathbf{M}\phi = \mathbf{w}$, we are almost ready to solve our original problem (1.21), or $\mathbf{T}\hat{\phi} = \mathbf{w}$. Recall that $\mathbf{T} = \mathbf{M} + \mathbf{\Delta T}$, where the matrix $\mathbf{\Delta T}$ represents the change from matrix $\mathbf{M}$ to $\mathbf{T}$. In our system, matrix $\mathbf{T}$ differs from $\mathbf{M}$ in exactly one element, $\mathbf{M_{k^*+1,k^*+1}}$. That one difference corresponds to the equations (1.21) and (1.22) when $k = k^* + 1$. When $k = k^* + 1$ in (1.22),

$$-\alpha_{k^*+1}\phi_{k^*+2} + (1 + \alpha_{k^*+1} + \alpha_{k^*})\phi_{k^*+1} - \alpha_{k^*}\phi_k^* = -a \tag{3.1}$$

and in our problem (1.21)

$$-\alpha_{k^*+1}\phi_{k^*+2} + (-1 + \alpha_{k^*+1} + \alpha_{k^*})\phi_{k^*+1} - \alpha_{k^*}\phi_k^* = -a. \tag{3.2}$$

For our system of equations $\mathbf{T}\hat{\phi} = \mathbf{w}$ we need entry $\mathbf{T_{k^*+1,k^*+1}} = (-1 + \alpha_{\mathrm{k^*+1}} + \alpha_{\mathrm{k^*}}) = (1 + \alpha_{\mathrm{k^*+1}} + \alpha_{\mathrm{k^*}}) - 2 = \mathbf{M_{k^*+1,k^*+1}} - 2$. So for us,

$$(\mathbf{\Delta T})_{\mathbf{ij}} = \begin{cases} -2 & i = j = k^* + 1 \\ 0 & \text{otherwise.} \end{cases}$$

We can also write $\mathbf{\Delta T} = \mathbf{yz^T}$ by setting

$$\mathbf{y} = -2\mathbf{e_{k^*+1}} \qquad \text{and} \qquad \mathbf{z} = \mathbf{e_{k^*+1}}. \tag{3.3}$$

where $\mathbf{e_{k^*+1}}$ is an infinite vector with zeros in every entry except at the $(\mathbf{k^* + 1})^{\mathbf{st}}$ entry where it is equal to one. Thus, $\mathbf{T} = (\mathbf{M} + \mathbf{\Delta T}) = \mathbf{M} + \mathbf{yz^T}$. It is necessary to write $\mathbf{\Delta T} = \mathbf{yz^T}$ because

the Sherman-Morrison formula is

$$\mathbf{T}\hat{\phi} = \mathbf{w} \;\Rightarrow\; \hat{\phi} = \mathbf{T^{-1}w} = (\mathbf{M} + \mathbf{yz^T})^{-1}\mathbf{w} = \mathbf{M^{-1}w} - \frac{\mathbf{M^{-1}yz^TM^{-1}w}}{\mathbf{1} + \mathbf{z^TM^{-1}y}}. \tag{3.4}$$

We have almost all of the information necessary to solve for $\hat{\phi}$ since we know $\mathbf{z}, \mathbf{y}, \text{and } \mathbf{M^{-1}w}$ which is the general solution for ϕ_k computed in Chapter 2. The only missing piece of the formula is $\mathbf{M^{-1}y}$.

If we define $\mathbf{x} = [\ldots\ \mathbf{x_{k-1}}\ \mathbf{x_k}\ \mathbf{x_{k+1}}\ \ldots]^\mathbf{T}$, then $\mathbf{Mx} = \mathbf{y}$ corresponds to the following equation

$$-\alpha_k x_k + (1 + \alpha_k + \alpha_{k-1})x_k - \alpha_{k-1}x_{k-1} = y_k \quad \forall k \in \mathbb{Z} \tag{3.5}$$

where

$$y_k = \begin{cases} -2 & k = k^* + 1 \\ 0 & k \neq k^* + 1 \end{cases} \tag{3.6}$$

This is another Jacobi operator system and we can use the method outlined in [7] to evaluate $\mathbf{x} = \mathbf{M^{-1}y}$. We consider (3.5) with homogeneous diffusion and inhomogeneous diffusion.

3.1 Homogeneous Diffusion

To consider (3.5) with homogeneous diffusion we set $\alpha_k = \alpha$ for all $k \in \mathbb{Z}$ to get

$$-\alpha x_{k+1} + (2\alpha + 1)x_k - \alpha x_{k-1} = y_k, \qquad \forall k \in \mathbb{Z}. \tag{3.7}$$

Once again, we are dealing with a second order difference equation which will have a general solution made up of two fundamental solutions and one particular solution. The homogeneous

equation for (3.7) is the same equation as the homogeneous equation for (2.2) in Chapter 2. Thus, (3.7) will have the same fundamental solutions, (2.8), as those that we constructed for (2.2) in Chapter 2.

The general solution takes the form

$$x_k = x_{k^*}\rho(k-k^*) + x_{k^*+1}\sigma(k-k^*) + \begin{cases} \frac{-1}{\alpha}\sum_{j=k^*+1}^{k} y_j\sigma(k-j) & k > k^* \\ 0 & k = k^* \\ \frac{1}{\alpha}\sum_{j=k}^{k^*} y_j\sigma(k-j) & k < k^* \end{cases} \tag{3.8}$$

which can be simplified by plugging in y_k from (3.6) which gives us

$$x_k = x_{k^*}\rho(k-k^*) + x_{k^*+1}\sigma(k-k^*) + \begin{cases} \frac{2}{\alpha}\sigma(k-1) & k > k^* \\ 0 & k \leq k^*. \end{cases} \tag{3.9}$$

We implement the following boundary conditions on x_k:

$$\lim_{k\to-\infty} x_k = \lim_{k\to\infty} x_k = 0 \tag{3.10}$$

and we use these to solve for coefficients x_{k^*} and x_{k^*+1}. We choose these boundary conditions in order to satisfy our original boundary conditions (1.9) for $\mathbf{T}\hat{\phi} = \mathbf{w}$. Recall that we are computing the solutions x_k to "correct" the solutions ϕ_k at the point ϕ_{k^*+1}. By setting the boundary conditions (3.10), we are ensuring that x_k will not affect the solutions $\hat{\phi}_k$ as $k \to \pm\infty$. Since we are dealing with homogeneous diffusion, we once again assume $k^* = 0$ without loss in generality.

As $k \to -\infty$

$$x_k = \frac{\lambda^{-k}}{\lambda - \lambda^{-1}}\Big(\lambda x_0 - x_1\Big) - \frac{\lambda^{k}}{\lambda - \lambda^{-1}}\Big(\lambda^{-1} x_0 - x_1\Big) = 0$$

and we require

$$\lambda x_0 - x_1 = 0. \tag{3.11}$$

As $k \to \infty$

$$x_k = \frac{\lambda^{-k}}{\lambda - \lambda^{-1}}\Big(\lambda x_0 - x_1 - \frac{2\lambda}{\alpha}\Big) - \frac{\lambda^{k}}{\lambda - \lambda^{-1}}\Big(\lambda^{-1} x_0 - x_1 - \frac{2\lambda^{-1}}{\alpha}\Big) = 0,$$

and we need

$$\lambda^{-1} x_0 - x_1 - \frac{2\lambda^{-1}}{\alpha} = 0. \tag{3.12}$$

We use 3.11 and 3.12 to solve for x_0 and x_1 and we find

$$x_0 = \frac{-2(1-\lambda^{-1})}{\lambda + 1} \qquad \text{and} \qquad \mathrm{x}_1 = \frac{-2(\lambda - 1)}{\lambda + 1}. \tag{3.13}$$

If we plug these coefficients back into (3.9) the general solution simplifies to

$$x_k = \begin{cases} x_1 \lambda^{1-k} & k > 0 \\ x_0 \lambda^{k} & k \leq 0. \end{cases} \tag{3.14}$$

Now that we have solutions $x_k = \mathbf{M^{-1}y}$ we can evaluate $\hat{\phi} = \mathbf{T^{-1}w}$ by plugging $\mathbf{M^{-1}w}$ and $\mathbf{M^{-1}y}$ into (3.4). First, notice that $1 + \mathbf{z^T M^{-1} y}$ and $\mathbf{z^T M^{-1} w}$ are scalars.

$$1 + \mathbf{z^T M^{-1} y} = 1 + [\cdots 0\, 1\, 0 \cdots] \begin{bmatrix} \vdots \\ x_0 \\ x_1 \\ x_2 \\ \vdots \end{bmatrix} = 1 + \mathrm{x}_1 \tag{3.15}$$

and

$$\mathbf{z^T M^{-1} w} = [\cdots\ 0\,1\,0\ \cdots] \begin{bmatrix} \vdots \\ \phi_0 \\ \phi_1 \\ \phi_2 \\ \vdots \end{bmatrix} = \phi_1. \tag{3.16}$$

Thus, according to the Sherman-Morrison formula,

$$\begin{aligned} \hat{\phi} = \mathbf{M^{-1} w} - \frac{\mathbf{M^{-1} y z^T M^{-1} w}}{\mathbf{1} + \mathbf{z^T M^{-1} y}} &= \phi_k - \frac{\phi_1 x_k}{1 + x_1} \\ &= \begin{cases} \lambda^{1-k}(\phi_1 - 1) + 1 & k > 0 \\ \lambda^k \phi_0 & k \leq 0 \end{cases} - \frac{\phi_1}{1 + x_1} \begin{cases} \lambda^{1-k} x_1 & k > 0 \\ \lambda^k x_0 & k \leq 0. \end{cases} \\ &= \begin{cases} 1 + \lambda^{1-k}(\phi_1 - 1 - \frac{\phi_1 x_1}{1+x_1}) & k > 0 \\ \lambda^k(\phi_0 - \frac{\phi_1 x_0}{1+x_1}) & k \leq 0 \end{cases} \end{aligned}$$

Recall that $\phi_1 = \lambda\phi_0$, and that $x_1 = \lambda x_0$. Then we can reduce the above equation to:

$$\hat{\phi}_k = \begin{cases} 1 + \lambda^{1-k}(\phi_1(\frac{1}{1+x_1}) - 1) & k > 0 \\ \lambda^k \phi_0(\frac{1}{1+x_1}) & k \leq 0 \end{cases} \tag{3.17}$$

where the coefficients ϕ_0, ϕ_1, x_0, and x_1 are as defined in (2.13) and (3.13). With these solutions for $\hat{\phi}_k$ in (3.17) we examine the interval of propagation failure in section 3.3 at the end of this chapter.

3.2 Inhomogeneous Diffusion

We find solutions to

$$-\alpha_k x_k + (1 + \alpha_k + \alpha_{k-1})x_k - \alpha_{k-1}x_{k-1} = y_k \quad \forall k \in \mathbb{Z} \tag{3.18}$$

when diffusion is inhomogeneous and there is one defect at α_0. Recall that the homogeneous equation for (3.18) is the same as the homogeneous equation of (2.15). Thus, the fundamental solutions for (3.18) will be the same fundamental solutions for (2.15) found in Chapter 2. Plugging in the values of y_k into (3.8), the general solution for inhomogeneous diffusion is

$$x_k = x_{k^*}\tilde{\rho}(k, k^*) + x_{k^*+1}\tilde{\sigma}(k, k^*) + \begin{cases} \frac{2}{\alpha}\tilde{\sigma}(k, k^* + 1) & k > k^* \\ 0 & k \leq k^*. \end{cases} \tag{3.19}$$

As in Chapter 2, we solve (3.18) for $k^* = -1$ and $k^* = 0$ because we wish to explore how adding a defect changes the interval of propagation failure when the front is at the defect and directly after it.

3.2.1 Fronts at the Defect

To consider stationary fronts at the defect, we set $k^* = -1$. Thus the general solution is

$$x_k = x_{-1}\tilde{\rho}(k, -1) + x_0\tilde{\sigma}(k, -1) + \begin{cases} \frac{2}{\alpha_0}\tilde{\sigma}(k, 0) & k > -1 \\ 0 & k \leq -1 \end{cases} \tag{3.20}$$

We use the same boundary conditions (3.10) and as $k \to -\infty$,

$$x_k = \frac{\lambda^{-k}}{\lambda - \lambda^{-1}}(x_{-1} - \lambda^{-1}x_0) - \frac{\lambda^k}{\lambda - \lambda^{-1}}(x_{-1} - \lambda x_0).$$

Then we need

$$x_{-1} - \lambda^{-1}x_0 = 0. \tag{3.21}$$

As $k \to \infty$,

$$\begin{aligned} x_k =& \frac{\lambda^{-k}}{\tau(\lambda - \lambda^{-1})}((\lambda\nu - \lambda^2)x_{-1} + (\lambda^2\nu - \lambda(\nu^2 - \tau^2))x_0 + \frac{2\tau}{\alpha_0}(\lambda^2 - \lambda\nu)) \\ & - \frac{\lambda^k}{\tau(\lambda - \lambda^{-1})}((\lambda^{-1}\nu - \lambda^{-2})x_{-1} + (\lambda^{-2}\nu - \lambda^{-1}(\nu^2 - \tau^2))x_0 + \frac{2\tau}{\alpha_0}(\lambda^{-2} - \lambda^{-1}\nu)). \end{aligned}$$

We require

$$(\lambda^{-1}\nu - \lambda^{-2})x_{-1} + (\lambda^{-2}\nu - \lambda^{-1}(\nu^2 - \tau^2))x_0 + \frac{2\tau}{\alpha_0}(\lambda^{-2} - \lambda^{-1}\nu) = 0. \tag{3.22}$$

Using 3.21 and 3.22 we solve for x_{-1} and x_0 and

$$x_{-1} = \frac{2(\lambda + \tau - 1)}{\alpha(-\lambda^3 + 2\lambda^2 - 2\lambda^2\tau + 2\lambda\tau - \lambda))} \qquad x_0 = \frac{2\lambda(\lambda + \tau - 1)}{\alpha(-\lambda^3 + 2\lambda^2 - 2\lambda^2\tau + 2\lambda\tau - \lambda)}, \tag{3.23}$$

and the general solution reduces to

$$x_k = \begin{cases} \frac{\lambda^{1-k}\tau x_0}{\lambda + \tau - 1} & k > 0 \\ \lambda^{k+1}x_{-1} & k \leq 0. \end{cases} \tag{3.24}$$

Now that we have evaluated $\phi = \mathbf{M^{-1}w}$ and $\mathbf{x} = \mathbf{M^{-1}y}$ we can evaluate $\hat{\phi} = \mathbf{T^{-1}w}$ using the Sherman-Morrison formula and

$$\hat{\phi}_k = \begin{cases} 1 + \frac{\lambda^{1-k}\tau}{\lambda+\tau-1}(\frac{\phi_0}{1+x_0} - 1) & k > 0 \\ \lambda^{k+1}\phi_{-1}(\frac{1}{1+x_0}) & k \leq 0. \end{cases} \tag{3.25}$$

Thus (3.25) is the solution to (1.21) when there is one defect at α_0 and the front is at the defect. We use (3.25) to calculate the interval of propagation failure in section 3.3.

3.2.2 Fronts After the Defect

When $k^* = 0$ we have

$$x_k = x_0\tilde{\rho}(k,0) + x_1\tilde{\sigma}(k,0) + \begin{cases} \frac{2}{\alpha}\tilde{\sigma}(k,1) & k > 0 \\ 0 & k \leq 0. \end{cases} \tag{3.26}$$

and we employ the same boundary conditions from (3.10) which we use to solve for the coefficients x_0 and x_1. As $k \to -\infty$

$$x_k = \frac{\lambda^{-k}}{\lambda - \lambda^{-1}}\Big(x_0(\nu - \lambda^{-1}) - \tau x_1\Big) - \frac{\lambda^k}{\lambda - \lambda^{-1}}\Big(x_0(\nu - \lambda) - \tau x_1\Big). \tag{3.27}$$

Recalling that $\nu = \lambda + \lambda^{-1} + \tau - 1$ we set

$$x_0(\nu - \lambda^{-1}) - \tau x_1 = 0 \quad \Leftrightarrow \quad x_0(\lambda + \tau - 1) - \tau x_1 = 0. \tag{3.28}$$

As $k \to \infty$

$$x_k = \frac{\lambda^{-k}}{\lambda - \lambda^{-1}}\Big(x_1\lambda(\lambda - \nu) - \lambda\tau x_0 - \frac{2\lambda}{\alpha}\Big) - \frac{\lambda^k}{\lambda - \lambda^{-1}}\Big(x_1\lambda^{-1}(\lambda^{-1} - \nu) - \lambda^{-1}\tau x_0 - \frac{2\lambda^{-1}}{\alpha}\Big)$$

and we need

$$x_1(\nu - \lambda^{-1}) - \tau x_0 + \frac{2}{\alpha} = 0 \quad \Leftrightarrow \quad x_1(\lambda + \tau - 1) - \tau x_0 = \frac{-2}{\alpha}. \tag{3.29}$$

Using 3.29 and 3.28 we solve for x_0 and x_1, giving

$$x_0 = \frac{-2\tau(1 - \lambda^{-1})}{\lambda + 2\tau - 1} \quad \text{and} \quad \mathrm{x}_1 = \frac{-2(1 - \lambda^{-1})(\lambda + \tau - 1)}{\lambda + 2\tau - 1}. \tag{3.30}$$

Plugging the coefficients back into (3.26) the general solution simplifies to

$$x_k = \begin{cases} \lambda^{1-k} x_1 & k > 0 \\ \lambda^k x_0 & k \leq 0. \end{cases} \tag{3.31}$$

Now that we have evaluated $\phi = \mathbf{M^{-1}w}$ and $\mathbf{x} = \mathbf{M^{-1}y}$ we can evaluate $\hat{\phi} = \mathbf{T^{-1}w}$.

$$\hat{\phi}_k = \begin{cases} 1 + \lambda^{1-k}(\phi_1(\frac{1}{1+x_1}) - 1) & k > 0 \\ \lambda^k(\phi_0 - \frac{\phi_1}{1+x_1} x_0) & k \leq 0 \end{cases} \tag{3.32}$$

where ϕ_0 andϕ_1 are found in (2.34) and x_0 and x_1 are in (3.30).Thus (3.32) is the solution for (1.21) in the case where there is one defect at α_0 and the front lies at the defect, $k^* = 0$.

Once again, we will use the formula for $\hat{\phi}_k$ in (3.32) to calculate the interval of propagation failure in the following section 3.3.

3.3 Interval of Propagation Failure

The interval of propagation failure for each α is determined by conditions (1.15), (1.16), and (1.17) because they guarantee solutions to the steady-state equation. The interval is the range of a values that satisfy all of these conditions. We first consider the interval of propagation failure for homogeneous diffusion, for which we chose we chose $k^* = 0$. Given this value of k^* conditions (1.15), (1.16), and (1.17) are

$$\hat{\phi}_0 \leq a/2 \tag{3.33}$$

$$a/2 < \hat{\phi}_1 < (a+1)/2 \tag{3.34}$$

$$(a+1)/2 \leq \hat{\phi}_2 \tag{3.35}$$

where $\hat{\phi}_0$, $\hat{\phi}_1$, and $\hat{\phi}_2$ are computed using (3.17). To find the interval of propagation failure, we plug in $\hat{\phi}_0$, $\hat{\phi}_1$ and $\hat{\phi}_2$ found in Table 3.1 into (3.33), (3.34), (3.35) and solve the inequalities for a. First we do this for homogeneous diffusion.

Table 3.1: Formulas for ϕ_0, ϕ_1, and ϕ_2 when diffusion is homogeneous. These values of $\hat{\phi}_k$ determine the interval of propagation failure.

Homogeneous Diffusion
$\hat{\phi}_0 = \frac{(a(\lambda^{-1}-1)+\lambda^{-1})}{3-\lambda}$
$\hat{\phi}_1 = \frac{(a(1-\lambda)+1)}{3-\lambda}$
$\hat{\phi}_2 = 1 + \frac{\lambda^{-1}(a(1-\lambda)-2+\lambda)}{3-\lambda}$

When solving the inequalities, we must consider any singularities with respect to α in the denominators of $\hat{\phi}_0$, $\hat{\phi}_1$ and $\hat{\phi}_2$, and any singularities in the solution for a. The denominators of ϕ_k

for $k = 0, 1, 2$ are equal to $3 - \lambda$. Recall that $\lambda = 1 + \frac{1}{2\alpha} + \frac{\sqrt{4\alpha+1}}{2\alpha}$; thus a singularity occurs when $\lambda = 3$ which implies $\alpha = 3/4$. The solutions for a from (3.33) and (3.35) contain another singularity when $5 - \lambda - 2\lambda^{-1} = 0$, or when $\alpha = \frac{7-\sqrt{17}}{8} \approx .3596$. The importance of these singularities is that the direction of each inequality symbol changes when solving for a in (3.33), (3.34), (3.35) once α crosses $3/4$ and $\frac{7-\sqrt{17}}{8}$. These changes are demonstrated in Table 3.2.

Table 3.2: Interval of Propagation Failure for Homogeneous Diffusion: Solutions to (3.33)-(3.34) for homogeneous diffusion.

Condition	$\alpha < \frac{7-\sqrt{17}}{8}$	$\frac{7-\sqrt{17}}{8} < \alpha < 3/4$	$\alpha > 3/4$	Color/Style on Graph
$\hat{\phi}_0 \leq a/2$	$\frac{2\lambda^{-1}}{5-\lambda-2\lambda^{-1}} \leq a$	$\frac{2\lambda^{-1}}{5-\lambda-2\lambda^{-1}} \geq a$	$\frac{2\lambda^{-1}}{5-\lambda-2\lambda^{-1}} \leq a$	Blue/solid line
$a/2 < \hat{\phi}_1 < (a+1)/2$	$\frac{2}{\lambda+1} < a < \frac{\lambda-1}{\lambda+1}$	$\frac{2}{\lambda+1} < a < \frac{\lambda-1}{\lambda+1}$	$\frac{\lambda-1}{\lambda+1} < a < \frac{2}{\lambda+1}$	Red/ crosses(+)
$\hat{\phi}_2 \geq (a+1)/2$	$a \leq \frac{5-4\lambda^{-1}-\lambda}{5-\lambda-2\lambda^{-1}}$	$a \geq \frac{5-4\lambda^{-1}-\lambda}{5-\lambda-2\lambda^{-1}}$	$a \leq \frac{5-4\lambda^{-1}-\lambda}{5-\lambda-2\lambda^{-1}}$	Blue/solid line

The intersection of all four inequalities is the interval of propagation failure. It is difficult to see the intersection simply by looking at the inequalities in Table 3.2, so we plot all four conditions as a function of α in the left panel of Figure 3.1 and graphically determine their intersection. The intersection of the inequalities lies between the red lines with crosses (+) for $\alpha < 3/4$ and between the blue lines for $\alpha > 3/4$. This means that for $\alpha < 3/4$, the condition (3.34) determines the interval of propagation failure, and that (3.33) and (3.35) determine the interval for $\alpha > 3/4$. Just the intersection of the conditions for the interval of propagation failure are plotted in the right panel of Figure 3.1.

The figure tells us that for small values of α, any value of a yields a front that fails to propagate. As α increases, the interval grows smaller until it converges to a single value of $a = 1/2$ as $\alpha \to 3/4$. For $\alpha > 3/4$, the interval of propagation failure exists only for values of a very close to $1/2$.

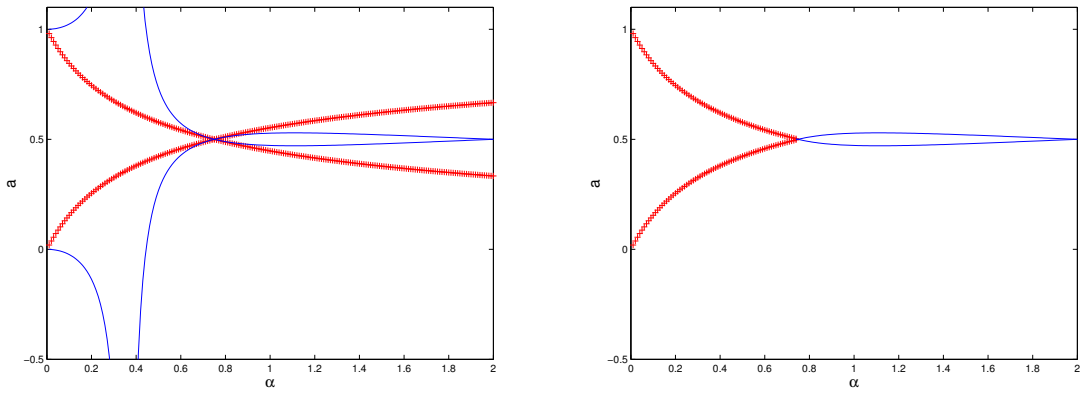

Figure 3.1: The interval of propagation failure with homogeneous diffusion. The left panel displays all four conditions 3.33-3.35, while the right panel plots only the conditions that determine the interval for given α.

According to Elmer [5], this value of $\alpha = 3/4$ is the maximum value of α for which stationary fronts exist for homogeneous diffusion when there is one $\hat{\phi}_k \in (\frac{a}{2}, \frac{a+1}{2})$. Recall the **Remark** made in Chapter 1. If we were to include more $\hat{\phi}_k$ nodes in between $(a/2, (a+1)/2)$ then we would need to resolve $\mathrm{M}\phi = \mathbf{w}$ when $n \geq 1$.

Our interval of propagation failure for homogeneous diffusion corresponds to Elmer's [5] interval of propagation failure. Because our results are comparable to Elmer's, this validates our method of using Jacobi operator theory and the Sherman-Morrison formula to construct solutions.

Now we consider the interval of propagation failure when one defect is present and the front is at

the defect, $k^* = -1$. When $k^* = -1$, the conditions (1.15), (1.16) and (1.17) are

$$\hat{\phi}_{-1} \leq a/2 \tag{3.36}$$

$$a/2 < \hat{\phi}_0 < (a+1)/(2) \tag{3.37}$$

$$(a+1)/2 \leq \hat{\phi}_1. \tag{3.38}$$

The formulas for the nodes $\hat{\phi}_{-1}$, $\hat{\phi}_0$ and $\hat{\phi}_1$ are computed using (3.25) and are listed in Table 3.3. We find the interval of propagation failure by plugging the formulas in Table 3.3 into (3.36), (3.37), and (3.38) and solving for a. The solutions, taking into account any singularities in $\hat{\phi}_{-1}$, $\hat{\phi}_0$, and $\hat{\phi}_1$ and in the solutions of a, are listed in Tables 3.4-3.6.

Table 3.3: Formulas for ϕ_{-1}, ϕ_0, and ϕ_1 when diffusion is inhomogeneous and $k^* = -1$. These values of ϕ_k determine the interval of propagation failure.

Inhomogeneous Diffusion
$\hat{\phi}_{-1} = \frac{a(\lambda+\tau-1)-\alpha_0(\lambda-1)}{\alpha(-\lambda^3+2\lambda^2-2\lambda^2\tau+2\lambda\tau-\lambda)+2\lambda(\lambda+\tau-1)}$
$\hat{\phi}_0 = \frac{\lambda(a(\lambda+\tau-1)-\alpha_0(\lambda-1))}{\alpha(-\lambda^3+2\lambda^2-2\lambda^2\tau+2\lambda\tau-\lambda)+2\lambda(\lambda+\tau-1)}$
$\hat{\phi}_1 = 1 + \frac{\tau}{\lambda+\tau-1}(\frac{\lambda(a(\lambda+\tau-1)-\alpha_0(\lambda-1))}{\alpha(-\lambda^3+2\lambda^2-2\lambda^2\tau+2\lambda\tau-\lambda)+2\lambda(\lambda+\tau-1)} - 1)$

Table 3.4: Solution to sufficiency condition (3.36) when $k^* = -1$, front is at the defect.

Condition	$\tau < \frac{\alpha\lambda^2-\alpha\lambda-2\lambda+2}{2-2\lambda\alpha}$	Color/Style on Graph
$\hat{\phi}_{-1} \leq \frac{a}{2}$	$\frac{-2\alpha_0(\lambda-1)}{\alpha(-\lambda^3+2\lambda^2-2\lambda^2\tau+2\lambda\tau-\lambda)+2(\lambda+\tau-1)(\lambda-1)} \leq a$	Blue/Solid line
	$\tau > \frac{\alpha\lambda^2-\alpha\lambda-2\lambda+2}{2-2\lambda\alpha}$	
	$\frac{-2\alpha_0(\lambda-1)}{\alpha(-\lambda^3+2\lambda^2-2\lambda^2\tau+2\lambda\tau-\lambda)+2(\lambda+\tau-1)(\lambda-1)} \geq a$	

Recall that the interval of propagation failure is the intersection of the inequalities in Tables 3.4-3.6. The inequalities have been plotted in Figure 3.2 and Figure 3.3 as functions of $\tau = \frac{\alpha_0}{\alpha}$ for

fixed values of $\alpha = 1/2$ and $\alpha = 7/10$, respectively. We fixed $\alpha < 3/4$ because $3/4$ is the upper bound on α if we are considering (1.13) in the case of one node in between $(a/2, (a+1)/2))$ [5].

Table 3.5: Solution to sufficiency condition (3.37) when $k^* = -1$, front is at the defect.

Condition		Color/Style on Graph
$a/2 < \hat{\phi}_0 < (a+1)/2$	$\frac{-2\alpha_0\lambda(\lambda-1)}{\alpha(-\lambda^3+2\lambda^2-2\lambda^2\tau+2\lambda\tau-\lambda)} < a < \frac{-2\lambda\alpha_0(\lambda-1)-k}{k-2\lambda a(\lambda+\tau-1)}$	Red/crosses (+)

Table 3.6: Solution to sufficiency condition (3.38) when $k^* = -1$, front is at the defect.

Condition	$\tau < \frac{1}{\alpha} - \frac{\lambda}{2} - \frac{1}{2}$	Color/Style on Graph
$\hat{\phi}_1 \geq (a+1)/2$	$a \leq \frac{(\alpha(-\lambda^3+2\lambda^2-2\lambda^2\tau+2\lambda\tau-\lambda)+2\lambda(\lambda+\tau-1))(\lambda-\tau-1)-2\tau\alpha_0\lambda(\lambda-1)}{(\lambda+\tau-1)(\alpha(-\lambda^3+2\lambda^2-2\lambda^2\tau+2\lambda\tau-\lambda)+2\lambda(\lambda+\tau-1)-2\tau\lambda)}$	Blue/Solid line
	$\tau > \frac{1}{\alpha} - \frac{\lambda}{2} - \frac{1}{2}$	
	$a \geq \frac{(\alpha(-\lambda^3+2\lambda^2-2\lambda^2\tau+2\lambda\tau-\lambda)+2\lambda(\lambda+\tau-1))(\lambda-\tau-1)-2\tau\alpha_0\lambda(\lambda-1)}{(\lambda+\tau-1)(\alpha(-\lambda^3+2\lambda^2-2\lambda^2\tau+2\lambda\tau-\lambda)+2\lambda(\lambda+\tau-1)-2\tau\lambda)}$	

The left panels of Figures 3.2 and 3.3 plot all of the conditions necessary for the interval of propagation failure, while the right panels show only the intersection of those conditions. When α is fixed at $1/2$, the only condition determining the interval of propagation failure is (3.37). When α is fixed at $7/10$, the interval is determined by (3.36) and (3.37). This shows that the conditions representing the interval of propagation failure vary depending on the value of α.

The dotted lines in the right panel of Figures (3.2) and (3.3) represent the interval of propagation failure when diffusion is homogeneous, or $\alpha_0 = \alpha$. It is clear from Figures 3.2 and 3.3 that the interval of propagation failure shifts downward from the interval for homogeneous diffusion when we consider fronts at the defect.

Taking a closer look at Figure 3.2 when $\alpha = 1/2$, the shift at $k^* = -1$ suggests that $\exists a \in (0, 1)$ such that a yields a stationary fronts when $\alpha_0 = \alpha$ but it produces a traveling front when $\alpha_0 < \alpha$.

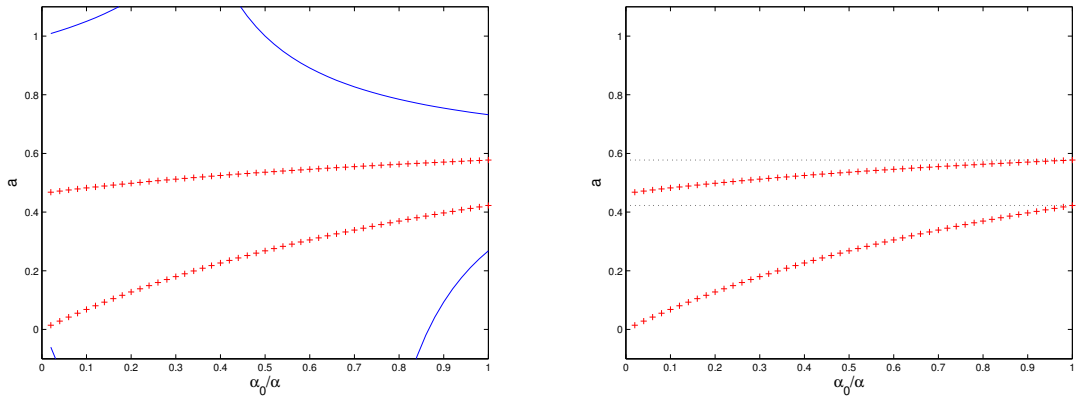

Figure 3.2: Interval of propagation failure when one defect is present at α_0, $k^* = -1$, and $\alpha = 1/2$.

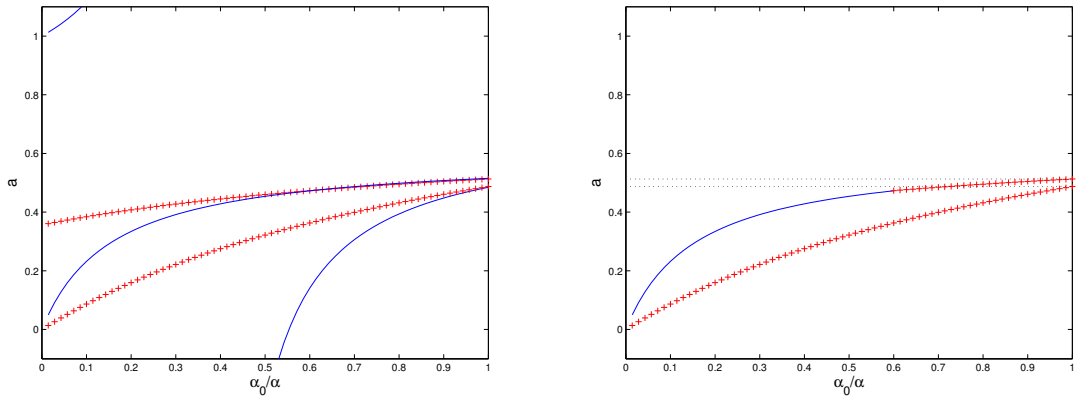

Figure 3.3: Interval of propagation failure when one defect is present at α_0, $k^* = -1$, and $\alpha = 7/10$.

Such values lie in between the upper red line (+) and the upper dotted black line in Figure 3.2. It may be that these values of a produce traveling fronts, but it is more realistic that the values yield stationary fronts for other monotonic fronts with different conditions than those outlined in our **Remark** in section 1.2. Figure 3.4 illustrates this theory, because the front is monotonic but contains no nodes in between $(a/2, (a+1)/2)$, thus $n = 0$. This could be a stationary front.

Also in Figure 3.2, $\exists a \in (0,1)$ such that a produces a traveling front when $\alpha_0 = \alpha$ but yields a stationary front when $\alpha_0 < \alpha$. These are the values of a that lie in between the bottom red line (+) and the bottom dotted black line, and this result is congruous with Theorem 3.2 in [7].

When α_0 is close to zero, this shift means that almost all left traveling waves become stuck at the defect because $a < 1/2$ indicates a left traveling front, and these values are included in the interval of propagation failure. Also, nearly all values of $a > 1/2$ lie outside the interval of propagation failure, hence, any right traveling front that has reached to $k = -1$ will propagate beyond the defect at α_0.

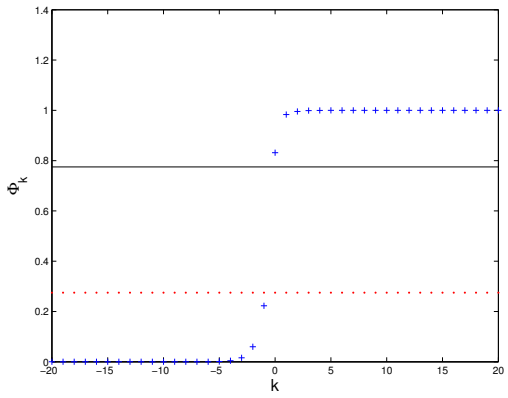

Figure 3.4: Monotonic front with conditions $a = .55$, $\alpha = 1/2$, and $\alpha_0 = .15$. According to Figure 3.2, this is a traveling front since $a = .55$ lies outside the interval of propagation failure when $\tau = .3$. The black solid line is the value $(a+1)/2$, the red dots represent $a/2$.

Examining Figure 3.3, the interval's shift downwards is even more drastic, and the interval is not as large for this larger value of α. This means there are fewer fronts satisfying our sufficiency condition in the **Remark** in section 1.2. Values of a that would produce a traveling front when $\alpha_0 = \alpha$, particularly values of $a < 1/2$, fail to propagate when a defect is added. Once again, nearly all values of $a > 1/2$ will produce a propagating front past $k = -1$.

Now we consider the interval of propagation failure when $k^* = 0$ (fronts to the right of the defect)

and the defect has been added at α_0. When $k^* = 0$ and diffusion is inhomogeneous, the conditions for (1.15), (1.16) and (1.17) are the same as (3.33), (3.34) and (3.35). The interval of propagation failure is found by plugging the values for $\hat{\phi}_{-1}$, $\hat{\phi}_0$ and $\hat{\phi}_1$, computed with (3.32), found in Table 3.7 into (3.33), (3.34) and (3.35), and solving for a. The solutions to these inequalities, with all singularities taken into account, are listed in Tables 3.8-3.10.

Table 3.7: Formulas for ϕ_0, ϕ_1, and ϕ_2 when diffusion is inhomogeneous and $k^* = 0$. These values of ϕ_k determine the interval of propagation failure.

Inhomogeneous Diffusion
$\hat{\phi}_0 = \frac{\tau(a(\lambda^{-1}-1)+\lambda^{-1})}{3-\lambda+2\lambda^{-1}\tau-2\lambda^{-1}}$
$\hat{\phi}_1 = \frac{(\lambda+\tau-1)(a(\lambda^{-1}-1)+\lambda^{-1})}{3-\lambda+2\lambda^{-1}\tau-2\lambda^{-1}}$
$\hat{\phi}_2 = 1+\lambda^{-1}[\frac{(\lambda+\tau-1)(a(\lambda^{-1}-1)+\lambda^{-1})}{3-\lambda+2\lambda^{-1}\tau-2\lambda^{-1}} - 1]$

Table 3.8: Solution to sufficiency condition (3.33) when diffusion is inhomogeneous and $k^* = 0$.

Condition	$\tau < \frac{\lambda}{2} - \frac{3}{2} + \lambda^{-1}$	$\tau > \frac{\lambda}{2} - \frac{3}{2} + \lambda^{-1}$	Color/Style on Graph
$\hat{\phi}_0 \leq a/2$	$a \geq \frac{2\tau\lambda^{-1}}{3-\lambda+2\tau-2\lambda^{-1}}$	$a \leq \frac{2\tau\lambda^{-1}}{3-\lambda+2\tau-2\lambda^{-1}}$	Blue/solid line

Table 3.9: Solution to sufficiency condition (3.34) when diffusion is inhomogeneous and $k^* = 0$.

Condition		Color/Style on Graph
$a/2 < \hat{\phi}_1 < (a+1)/2$	$\frac{2\lambda^{-1}(\lambda+\tau-1)}{\lambda+2\tau-1} < a < \frac{\lambda-1}{\lambda+2\tau-1}$	Red/ crosses (+)

Table 3.10: Solution to sufficiency condition (3.35) when diffusion is inhomogeneous and $k^* = 0$.

Condition	$\tau < \frac{5-6\lambda^{-1}-\lambda+2\lambda^{-2}}{2\lambda^{-2}-4\lambda^{-1}}$	$\tau > \frac{5-6\lambda^{-1}-\lambda+2\lambda^{-2}}{2\lambda^{-2}-4\lambda^{-1}}$	Color/Style on Graph
$\hat{\phi}_2 \geq (a+1)/2$	$a \leq \frac{5-6\lambda^{-1}-\lambda+2\lambda^{-2}(1+\tau-\tau\lambda)}{5-6\lambda^{-1}-\lambda+4\lambda^{-1}\tau+2\lambda^{-2}(1-\tau)}$	$a \geq \frac{5-6\lambda^{-1}-\lambda+2\lambda^{-2}(1+\tau-\tau\lambda)}{5-6\lambda^{-1}-\lambda+4\lambda^{-1}\tau+2\lambda^{-2}(1-\tau)}$	Blue/solid line

The solutions in Tables 3.8-3.10 are plotted in Figures 3.5 and 3.6 as functions of $\tau = \frac{\alpha_0}{\alpha}$ for fixed $\alpha = 1/2$ and $\alpha = 7/10$, respectively. The right panels of the figures show the intersection of the solutions to (3.33), (3.34) and (3.35) plotted versus the interval of propagation failure for homogeneous diffusion in the black dotted lines. The conditions that determine the interval of propagation failure differ between the two plots. In Figure 3.5, only (3.34) determines the interval, while in Figure 3.6, a combination of conditions (3.34) and (3.35) determine the interval.

It's obvious in Figures 3.5 and 3.6 that the interval of propagation failure has shifted upwards from the corresponding value of α in the interval for homogeneous diffusion. Thus when the defect is bad, or α_0 is close to zero, it appears that all fronts traveling to the left (when $a < 1/2$) travel past $k = 0$ because those values are below the interval of propagation failure. The only fronts that may become stuck are those traveling to the right, i.e. with detuning parameter $a > 1/2$. These results are incongruous with Theorem 3.2 in [7], which states that when k^* is after the defect and if $\exists a \in (0, 1)$ that yields a traveling front when $\alpha_0 = \alpha$ then there are no corresponding stationary fronts to a when $\alpha_0 < \alpha$.

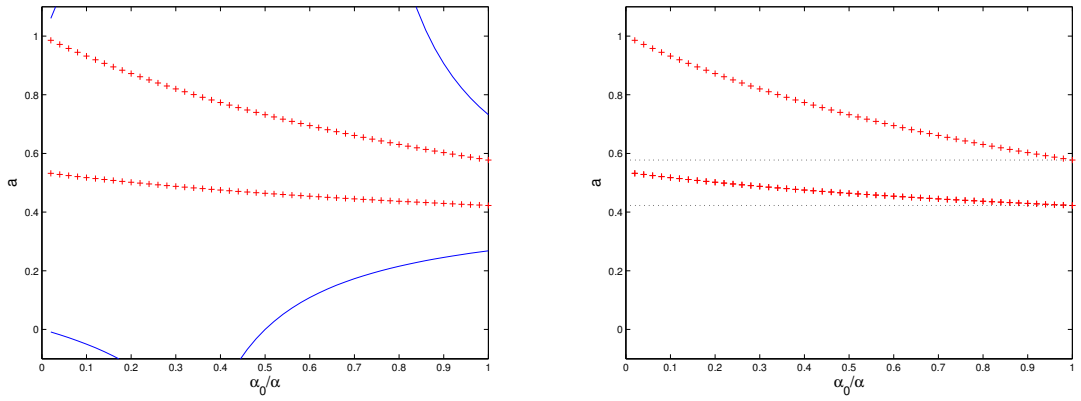

Figure 3.5: Interval of propagation failure when $k^* = 0$ when one defect is present at α_0 and $\alpha = 1/2$.

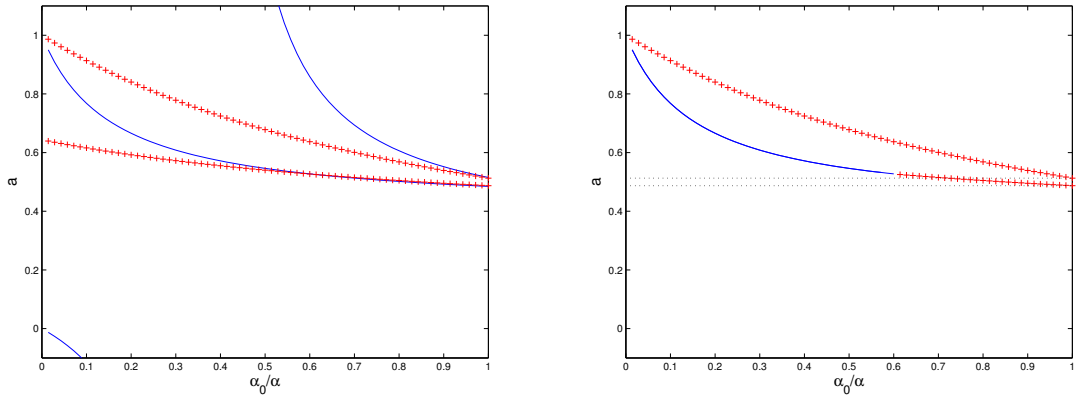

Figure 3.6: Interval of propagation failure when $k^* = 0$ when one defect is present at α_0 and $\alpha = 7/10$.

A comparison of the three intervals of propagation failure in Figures 3.7 and 3.8 sheds light onto these shifts in the intervals when the front is at and after the defect. When $\alpha_0/\alpha = 1/2$ in Figure 3.7, $a = .6$ is outside the red lines representing the interval of propagation failure for a front at the defect, thus any front with detuning parameter $a = .6$ will travel at $k = -1$. However, $a = .6$ is in between the blue lines representing the interval of propagation failure for fronts after the defect,

thus that same front will become stuck when $k^* = 0$. If $a = .6$ the front is right moving, so that front will become stuck at $k = 0$. Also, most left moving fronts (a¡1/2) become pinned at $k = -1$. Thus Figure 3.7 shows us that the interval of propagation failure is much worse than the interval of propagation failure when diffusion is homogeneous, because more fronts become stuck at either $k = -1$ or $k = 0$. The exception to this rule occurs when the defect is severe (α_0 is close to zero) and $a \approx 1/2$, where there is gap in between the blue (solid) and red (+) lines. This gap could represent other monotonic fronts that don't satisfy our condition in the **Remark** in section 1.2 but may also be stationary fronts.

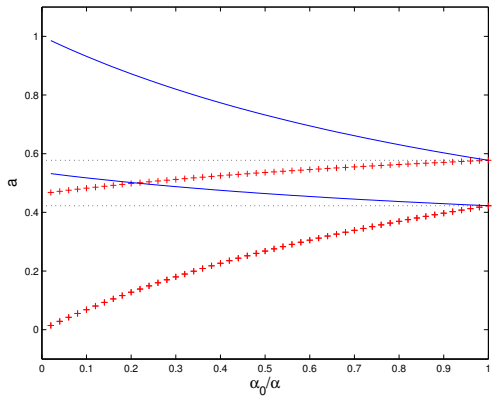

Figure 3.7: A comparison of the intervals of propagation failure when a defect is present at α_0 when the front is at the defect ($k^* = -1$, the red crosses (+)), after the defect ($k^* = 0$, the blue solid line), when α is fixed at $1/2$, and when diffusion is homogeneous (black dotted lines).

This region between the two intervals of propagation failure is even larger in Figure 3.8. The gap suggests values of a which yielded stationary fronts when diffusion was homogeneous (the values in between the dotted black lines) now produce fronts that travel past the defect (because they lie outside the red(+) lines) and past k=0 (because they lie outside the blue solid lines). However, Figure 3.9 shows a monotonic front after the defect ($k^* = 0$) in which $n = 2$ nodes lie in between $(a/2, (a+1)/2)$ and $a = 1/2$. Fronts satisfying our **Remark** from section 1.2, meaning $n = 1$, travel for values of a in the gap region. But Figure 3.9 could be showing us that when a lies

between the red (+) and blue lines, fronts for which $n = 2$ become pinned.

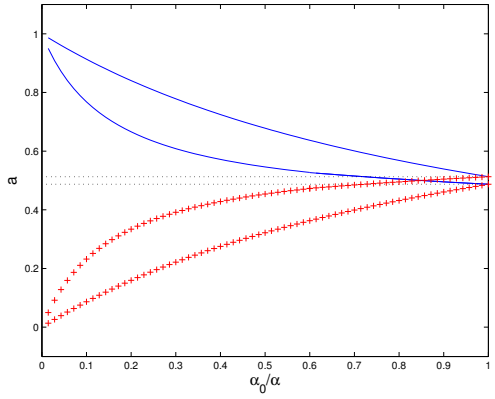

Figure 3.8: A comparison of the intervals of propagation failure for different k^* when a defect is present at α_0 and α is fixed at $7/10$. The red lines (+) represent the interval when $k^* = -1$, the blue solid line represents the interval when $k^* = 0$. The black lines (-) represent the interval when diffusion is homogeneous and $\alpha = 7/10$.

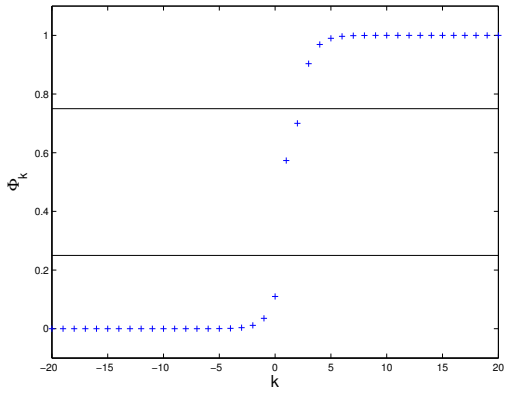

Figure 3.9: Monotonic front with conditions $a = .5$, $k^* = 0$, and $\alpha_0/\alpha = .5$. According to Figure 3.8, this is a traveling front since $a = .5$ lies outside the interval of propagation failure when $\alpha_0/\alpha = .5$. The black solid lines are, from bottom to top, $a/2$ and $(a+1)/2$.

The asymmetry of the interval of propagation failure when the front is after the defect is congruous with the results produced in [7]. However, the interval of propagation failure for fronts at the

defect is symmetrical in [7], whereas it is asymmetrical in our results. This is likely due to the restrictions we placed on (1.13) to include only one node in $(a/2, (a+1)/2)$, and our definition of k^*. /As Figure **??** suggests, if we allowed more nodes to fall in to that interval, or considered any monotonic front to be stationary regardless of the number of nodes in between $(a/2, (a+1)/2)$, we would probably see the symmetry in the interval of propagation failure.

The plots in this chapter show us that adding a defect will cause more fronts to become stationary at or right after the defect. Fronts traveling to the left could get stuck at $k = -1$, and fronts traveling to the right could become stationary at $k = 0$.

CHAPTER 4: SIMULATIONS

4.1 Comparison

The problem of finding the general solution for

$$-\alpha_k\phi_{k+1} + (v_k + \alpha_k + \alpha_{k-1})\phi_k - \alpha_{k-1}\phi_{k-1} = w_k \tag{4.1}$$

in which more than one defect is present is difficult to solve analytically. Even when we consider (4.1) in the case of just one defect at α_0, there are three different sets of fundamental solutions (2.17), (2.18), and (2.19), to derive because the fundamental solutions change based on whether k^* is less than, greater than, or equal to zero. When diffusion is inhomogeneous, it is interesting to consider other values of k^* because the interval of propagation failure changes as the proximity of k^* varies with respect to the defect region. If we were to consider m defects, we would have to compute $m+2$ different sets of fundamental solutions to account for the all of the varying positions of k^* relative to the defects. Once the fundamental solutions were computed, the general solutions would need to be solved for each of the $m+2$ cases as well, a doable yet time-consuming process.

Also, recall the **Remark** made in 1.2. It would be interesting to see what happens as we add more nodes n in between η_0 and η_1 in the nonlinearity f. If we chose to vary n, then we would have to solve another difference equation for each value of n.

The importance of the nonlinearity's role in determining the interval of propagation failure has already been stated in 1.1. Having a resource that quickly computes solutions to (1.3) with different nonlinearities would be helpful in comparing the affects that different nonlinearities have on the interval of propagation failure.

The scripts `SDNagumo.m` and `FundSol.m` were created in MATLAB so that we could quickly solve (1.3) when more defects are added, the value of n changes, or the nonlinearity changes. The details of how the scripts work is outlined in the next section, 4.2. In this section, we compare the algorithmic solutions with known exact solutions to examine the accuracy of the solutions derived with our scripts.

Remark: Let ψ represent the solutions to $\hat{\phi} = \mathbf{T}^{-1}\mathbf{w}$ that were computed using the scripts `SDNagumo.m` and `FundSol`.

Figures 4.1-4.3 were made comparing ψ to our formulas for the solution (3.17), when diffusion is homogeneous. The error in Figures 4.1 and 4.2 is taken to be the 2-norm of ψ and $\hat{\phi}$. Figure 4.1 tells us that the value of a affects the error in ψ very little while the value of α affects the error significantly. Figure 4.2 shows us that ψ is more reliable for values of α close to 1.

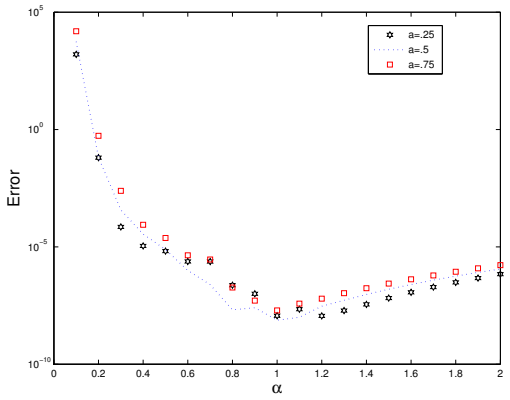

Figure 4.1: Error in ψ for fixed a as α varies.

The error in Figure 4.3 is the $|\hat{\phi}_k - \psi_k|$. Figure 4.3 tells us that the error for any a and α close to $k^* = 0$ is very good $\approx 10^{-15}$. This is important because these values of ψ_k can be used to help us determine the interval of propagation failure.

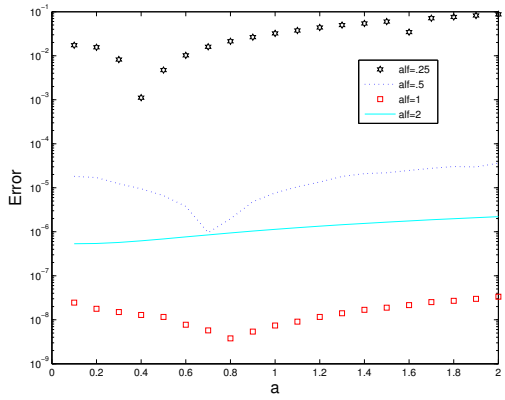

Figure 4.2: Error in ψ for fixed α as a varies.

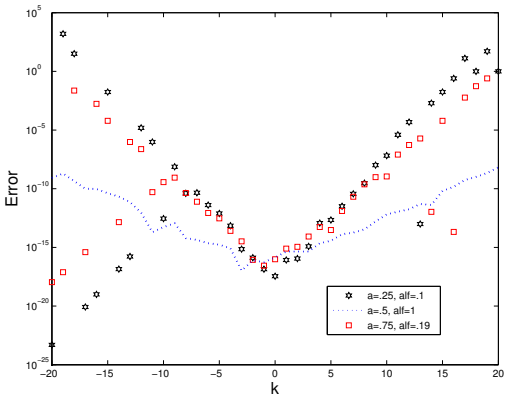

Figure 4.3: Error in ψ for different fixed values of a and α. The value of $k^* = 0$.

Figures 4.4 and 4.5 are plots of ψ compared to formula (3.25) from 3.2.2. The error in Figure 4.4 is taken to be the 2-norm and the error in Figure 4.5 is $|\hat{\phi} - \psi|$. Figure 4.4 demonstrates that adding a defect decreases the accuracy of ψ. Figure 4.5 shows us that the error of ψ_k close to $k^* = 0$ is very good, $\approx 10^{-16}$ for any α, α_0, and a. It is critical that nodes close to $\hat{\phi}_{k^*}$ are accurate since these nodes determine the interval of propagation failure.

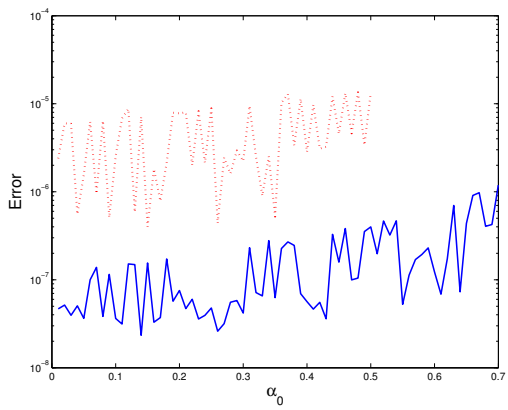

Figure 4.4: Error in ψ as α_0 varies. Red line represents $\alpha = 1/2$, blue line $\alpha = 7/10$.

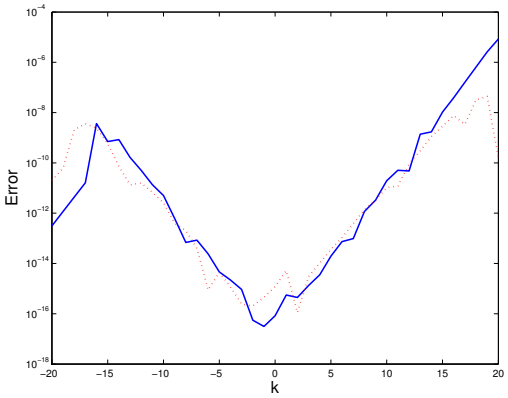

Figure 4.5: Error in ψ solutions in case of one defect. Blue line represents $\alpha = 1/2$ with $\alpha_0 = .25$ and $a = .6$, red line represents $\alpha = 7/10$ with $\alpha_0 = .42$ and $a = .6$, value of $k^* = 0$, values of α, α_0, and a were chosen from the interval of propagation failure (Figures 3.5 and 3.6) from section 3.3.

Figures 4.1-4.5 indicate that to achieve the most accurate results from the script, α should be kept close to 1. The figures also tell us that no matter what the parameter values are, the accuracy of ψ_k close to k^* is close to machine accuracy.

4.2 Code Description

We have designed two programs in MATLAB which work in tandem to produce solutions to (1.3) when $\dot{\phi}_j(t) = 0$. The first is a function called `FundSol.m` which outputs a matrix containing fundamental solutions for any location of k^*. The function follows the procedure outlined in Lemma 3.3 from [7] to achieve the solutions. The script `SDNagumo.m` calls the fundamental solutions from `FundSol` and uses them to create the particular solutions for $\phi = \mathbf{M^{-1}w}$ and $\mathbf{x} = \mathbf{M^{-1}y}$. Once the particular solutions are made, `SDNagumo.m` then solves for the coefficients $\phi_{k^*}, \phi_{k^*+1}, x_{k^*}$, and x_{k^*+1}, computes the general solution vectors ϕ and $\mathbf{x}$ and uses those vectors in the Sherman-Morrison formula to solve for the solution vector $\hat{\phi}_k$.

Note that when we set the right hand side of (1.22) equal to zero and solve for ϕ_{k+1} and ϕ_{k-1} we get the following two equations

$$\phi_{k+1} = \tfrac{1}{\alpha_k}((1 + \alpha_k + \alpha_{k-1})\phi_k - \alpha_{k-1}\phi_{k-1}) \tag{4.2}$$

$$\phi_{k-1} = \tfrac{1}{\alpha_{k-1}}((1 + \alpha_k + \alpha_{k-1})\phi_k - \alpha_k\phi_{k+1}). \tag{4.3}$$

Given initial conditions (2.16) for any starting point k^*, (4.2) and (4.3) give us formulas to derive the fundamental solutions recursively $\forall k$. The function `FundSol.m` takes a vector with the initial conditions for the fundamental solutions (2.16), and a vector containing the value of the diffusion coefficients α_k on the interval lattice and computes the fundamental solutions with formulas (4.2) and (4.3). Being able to manipulate the vector of diffusion coefficients is what allows us to examine (1.3) with multiple defects.

Recall that [12] gives us the particular solution

$$\begin{cases} \sum_{j=k^*+1}^{k} \frac{-1}{\alpha_j} w_j \tilde{\sigma}(k,j) & k > k^* \\ 0 & k = k^* \\ \sum_{j=k+1}^{k^*} \frac{1}{\alpha_j} w_j \tilde{\sigma}(k,j) & k < k^*. \end{cases} \tag{4.4}$$

to equation (2.1), and

$$\begin{cases} \sum_{j=k^*+1}^{k} \frac{-1}{\alpha_j} y_j \tilde{\sigma}(k-j) & k > k^* \\ 0 & k = k^* \\ \sum_{j=k}^{k^*} \frac{1}{\alpha_j} y_j \tilde{\sigma}(k-j) & k < k^* \end{cases} \tag{4.5}$$

to (3.5). The script `SDNagumo.m` first creates vectors for w_k and y_k, the right hand sides of the equations (2.1) and (3.5), that are k^* dependent. Being able to change these vectors is what allows us to consider different nonlinearities, different positions of k^*, and for our choice in nonlinearity, the varying number of n nodes in between η_0 and η_1. `SDNagumo.m` then makes another vector storing the particular solution for each value ϕ_k and x_k. Recall that we need to employ the boundary conditions to solve for the coefficients ϕ_{k^*}, ϕ_{k^*+1}, x_{k^*}, and x_{k^*+1}. That is, we are examining the general solution as $k \to \pm\infty$, or

$$\lim_{k\to\infty} \phi_k = \lim_{k\to\infty} (\tilde{\rho}(k,k^*)\phi_{k^*} + \tilde{\sigma}(k,k^*)\phi_{k^*+1} + \sum_{j=k^*+1}^{k} \frac{-1}{\alpha_j} w_j \tilde{\sigma}(k,j)) = 1. \tag{4.6}$$

and

$$\lim_{k\to-\infty} \phi_k = \lim_{k\to-\infty} (\tilde{\rho}(k,k^*)\phi_{k^*} + \tilde{\sigma}(k,k^*)\phi_{k^*+1} + \sum_{j=k+1}^{k^*} \frac{1}{\alpha_j} w_j \tilde{\sigma}(k,j)) = 0 \tag{4.7}$$

We obviously cannot take $k \to \pm\infty$ in our code, but we can compute the fundamental and particular solutions for a sufficiently large value of k. We kept $k = \pm 20$ as our largest and smallest node. Then we can use (4.6) and (4.7) to solve for the coefficients ϕ_{k^*} and ϕ_{k^*+1} by solving a 2×2

system of equations

$$\begin{bmatrix} \tilde{\rho}(20,k^*) & \tilde{\sigma}(20,k^*) \\ \tilde{\rho}(-20,k^*) & \tilde{\sigma}(-20,k^*) \end{bmatrix} \begin{bmatrix} \phi_{k^*} \\ \phi_{k^*+1} \end{bmatrix} = \begin{bmatrix} 1-\sum_{j=k^*+1}^{k} \frac{-1}{\alpha_j} w_j \tilde{\sigma}(k,j)) \\ -\sum_{j=k+1}^{k^*} \frac{1}{\alpha_j} w_j \tilde{\sigma}(k,j)) \end{bmatrix} \tag{4.8}$$

for $\begin{bmatrix} \phi_{k^*} \\ \phi_{k^*+1} \end{bmatrix}$ by using the matrix solver command in MATLAB. Once the coefficients are solved, we can compute the general solution $\forall \phi_k$,

$$\phi_k = \phi_{k^*}\tilde{\rho}(k,k^*) + \phi_{k^*+1}\tilde{\sigma}(k,k^*) + \begin{cases} \sum_{j=k^*+1}^{k} \frac{-1}{\alpha_j} w_j \tilde{\sigma}(k,j) & k > k^* \\ 0 & k = k^* \\ \sum_{j=k+1}^{k^*} \frac{1}{\alpha_j} w_j \tilde{\sigma}(k,j) & k < k^* \end{cases} \tag{4.9}$$

with all of our stored fundamental and particular solutions. We follow the same approach for x_k except we use the boundary conditions for (3.5), (3.10) to solve for the coefficients. MATLAB solves the following 2×2 matrix in order to evaluate the coefficients for x_{k^*} and x_{k^*+1}

$$\begin{bmatrix} \tilde{\rho}(20,k^*) & \tilde{\sigma}(20,k^*) \\ \tilde{\rho}(-20,k^*) & \tilde{\sigma}(-20,k^*) \end{bmatrix} \begin{bmatrix} x_{k^*} \\ x_{k^*+1} \end{bmatrix} = \begin{bmatrix} -\sum_{j=k^*+1}^{k} \frac{-1}{\alpha_j} y_j \tilde{\sigma}(k-j) \\ -\sum_{j=k}^{k^*} \frac{1}{\alpha_j} y_j \tilde{\sigma}(k-j). \end{bmatrix} \tag{4.10}$$

We can then evaluate $x_k \, \forall k$ by plugging in the coefficients, the fundamental solutions, and the particular solutions into

$$x_k = x_{k^*}\rho(k-k^*) + x_{k^*+1}\sigma(k-k^*) + \begin{cases} \frac{-1}{\alpha} \sum_{j=k^*+1}^{k} y_j \sigma(k-j) & k > k^* \\ 0 & k = k^* \\ \frac{1}{\alpha} \sum_{j=k}^{k^*} y_j \sigma(k-j) & k < k^*. \end{cases} \tag{4.11}$$

Once the script has the solutions for ϕ_k and x_k, all that is left to do in order to use the Sherman-

Morrison formula (3.4) is to make a vector $\mathbf{z^T}$. Once this vector is made, we have all that we require to use the Sherman-Morrison formula

$$\hat{\phi} = \mathbf{M^{-1}w} - \frac{\mathbf{M^{-1}yz^TM^{-1}w}}{\mathbf{1} + \mathbf{z^TM^{-1}y}}. \tag{4.12}$$

The code for `FundSol.m` and `SDNagumo` can be found in the appendix.

CHAPTER 5: CONCLUSION

We constructed exact monotonic steady-state solutions to (1.3) with a continuous piecewise nonlinearity f using Jacobi operator theory and the Sherman-Morrison formula, an original approach to this problem. Initial restrictions on the stationary front solutions (1.15), (1.16), and (1.17) revealed the interval of propagation failure in the case of homogeneous and inhomogeneous diffusion. Our results for the interval of propagation failure with homogeneous diffusion were corroborated by previous work done in [5]. The interval of propagation failure found when one defect is present is an original result. The result is important in helping us to understand how fronts propagate, or fail to propagate, when nerve cells are damaged by multiple sclerosis.

We examined the interval of propagation failure for fronts at and directly after a single defect, because the most significant changes to the interval occur when the front is close to the defect. This represents the conditions for which a front becomes stationary when just one node in the neuron has erosion of the myelin sheath. The interval tells us that when a defect is present, the interval of propagation failure worsens. That is, there exist fronts that would propagate under homogeneous conditions that become stuck at or right after the defect. Based off of similar experiments conducted in [7], we expected that the interval of propagation failure of fronts at the defect, would be symmetric about $a = 1/2$. This was not the case for our problem set-up. Perhaps the interval would be symmetric if we altered our restriction on n in **Remark** in section 1.2. If we considered any monotonic front to be a stationary front, the interval of propagation failure would encompass more values of a.

Because damage to the myelin sheath can occur at more than one node, we'd like to solve for exact solutions when a region of defects is present, or $\alpha_k \neq \alpha$ for $-p \leq k \leq q$ and $p, q \in \mathbb{Z}^+$. When one defect is present, we see that the interval of propagation failure expands, making it more difficult

for fronts to pass through the nerve. However, there is a hypothesis that when more than one defect exists in the axon, the interval of propagation failure may actually improve from when only one is present. This means that more impulses may propagate through an axon in which demyelination occurs at multiple parts of the nerve than when just one node is damaged. The case of multiple defects should be explored in future work in order to test this hypothesis.

The case of multiple defects is tedious to solve for exact solutions, thus we have presented an algorithmic method in MATLAB which calculates solutions to (1.3) in the case of more than one defect. The algorithmic script is capable of evaluating the steady-state solutions of (1.3) with different choices in nonlinearity f, and different cases of our own nonlinearity, i.e. varying values of n as defined in the **Remark** in section 1.2. The algorithm's accuracy varies based on choices in parameter values. Under certain parameter conditions, the algorithm yields solutions with machine accuracy. The threshold of parameter values for which the algorithm produces accurate results could be tested in future research.

Our contributions include: a new method for solving a reaction-diffusion equation with a continuous nonlinearity, a method for finding the interval of propagation failure for a class of solutions to the reaction-diffusion equation, and an algorithmic method capable of computing solutions to the Nagumo equation in MATLAB.

APPENDIX: CODE

The following code is the algorithmic approach to solving the general solutions to the spatially discrete Nagumo equation (1.3).

```
%%%%%%%%%The following code creates solutions for spatially discrete
%%%%%%%%%Nagumo equations with a piecewise nonlinearity.

clear %clears all variables

alf = .7; % value of diffusion coefficients alpha
bet = .42; % the value of the defects in the defective region.
N = 20;%half the total number of elements in soln vector
M = 0;%number of defects in alpha vector depends on M.
           %M=x corresponds to 2x+1 defects
a =.6;%value of a

% vector limits
nminus = 1;
nplus = 2*N +1; %size of the solution vector is (1 x 2N+1)
mminus = N +1 -M; %
mplus = N +1 +M;

% diffusion coefficients
beta = bet*ones(1,mplus+1-mminus); %sets defect interval to length
   %mplus+1-mminus
alpha(nminus:mminus-1) = alf*ones(1,mminus-1);
%sets interval of homogeneous diffusion before defect interval
alpha(mminus:mplus) = beta;%centers defect interval around zero
alpha(mplus+1:nplus) = alf*ones(1,nplus-mplus);
```

```
%interval of homogeneous diffusion after defect interval

%initial conditions for the fundamental solution
rho(1)=1;  rho(2)= 0;
sig(1)=0;  sig(2)= 1;

%the FundSol function creates the fundamental solutions with the given
%initial conditions and diffusion coefficient vector
[rhof, sigf]=FundSol(rho, sig, alpha, N);

%setting k0 and creating w_k vector. w_k represents the right hand side
% of the difference equation. When k0=N+1, this corresponds to the case
%that k*=0. For k0=x, this corresponds to k* = x-N-1.
k0=N+1;
w(1:k0)=0;
w(k0+1)= -a;
w(k0+2:nplus)= 1;

%creates particluar soln vector for all
psum=0;
for jk=k0+1:nplus
        for i=k0+1:jk
        par = psum + w(i)*(-1/(alpha(i)))*sigf(i, jk);
        psum= par;
        end
    part(jk-k0) = psum;
    psum=0;
```

```
end

ps=part(length(part));
%particular soln as k goes to "infinity". This is the last element
%in the particular soln vector
A=[rhof(k0,nplus) sigf(k0,nplus); rhof(k0,1) sigf(k0,1)];
%matrix of coefficients
b=[(1-ps); 0]; %matrix of constants
s=A\ b; %solves for coefficients phi0=s(1,1) and phi1=s(2,1)

phim= s(1,1)*rhof(k0, 1:k0) + s(2,1)*sigf(k0,1:k0);
%general soln for phi_k when k<=k0
phip= s(1,1)*rhof(k0, k0+1:nplus) + s(2,1)*sigf(k0,k0+1:nplus) + part;
%general soln for phi_k when k>k0
phi=[phim phip];
% combines phim and phip vectors into one containing solns
%phi_k for all k

%%%%%%%%%%%%%%%Now we have phi=M^-1*w %%%%%%%%%%
%%%%%%%%%%Time to compute x = M^-1*y %%%%%%%%%%%%
%%The fundamental solns are the same for Mx=y, thus all that's left is
%%to compute particular solns and determine coefficients x0 and x1%%%

%creating y_k vector, the right hand side of the difference equation
y(1:k0)=0; y(k0+1)= -2; y(k0+2:nplus)=0;

%makes particluar soln for x
```

```
xsum=0;
for j=k0+1:nplus
    for i=k0+1:j
        xpar= xsum + y(i)*(-1/alpha(i))*sigf(i,j);
        xsum= xpar;
    end
    xpart(j-k0) = xsum;
    xsum=0;
end

xps=xpart(length(xpart));
%particular soln as k goes to "infinity". This is last element in the
%particular soln vector
X=[rhof(k0,nplus) sigf(k0,nplus); rhof(k0,1) sigf(k0,1)];
%matrix of coefficients
y=[-xpart(length(xpart)); 0];
%matrix of constants determined by boundary conditions
xs=X \ y;
%solves for coefficients x0 and x1

x(1:k0)=xs(1,1)*rhof(k0, 1:k0)+xs(2,1)*sigf(k0, 1:k0);
%gen solns for x_k for k<=k0
x(k0+1:nplus)=xs(1,1)*rhof(k0,k0+1:nplus)+
   xs(2,1)*sigf(k0,k0+1:nplus)+xpart;
%gen solns for x_k for k>k0
```

```
%%%%Now that we have both phi=M^(-1)w and x=M^(-1)y, we can use these
%%%%solution vectors in the Sherman-Morrison formula to solve for
%%%%solns hatphi=T^(-1)w%%%%%%
z(1:k0)=0; z(k0+1)=1; z(k0+2:nplus)=0;
%creates vector z transpose for Sherman-Morrison formula
e=1+ z*x.';%scalar in the Sherman-Morrison formula
PHI= phi.' - (1/e)*((x.')*z*phi.');%The Sherman-Morrison formula
%%%%%%Now we have the solutions for hatphi=T^(-1)w%%%%%%%%
```

Code for computing the fundamental solutions is `Fundsol.m` .

```
Fundsol.m
function [rhof,sigf] = HMVVfunc1(rho,sig,alpha, N)
% Generates the functions rhof and sigf, the
% polynomial solutions of the homogeneous Jacobi
% operator equation for discontinuous nonlinearity.

for k0=1:2*N+1 %k0 is the equivalent of k*. The loop goes through each
               %each value of k0, 1-2N+1, and computes the fundamental
               %solns from that starting point. k0=x corresponds to
               %k* = x-N-1. Thus k0=1 corresponds to k* = -20.

%%%%%%% this 'if' loop for k0=1:2N %%%%%

if k0<2*N+1
%RHO0 and SIG0 are the fund soln vectors to the left of k0. The initial
%conditions must be stored at the elements k0 and k0+1 in the vectors,
%since the solns are computed backwards. That is, if k0=5, then the
```

```
%next fund solns we wish to find are rho(4) and sig(4). By keeping
%the initial conditions at the k0 and k0+1 elements, we allow
%room to work backwards to store the other fund solns in order.

RHO0(k0) = 1; RHO0(k0+1)=0;
SIG0(k0) = 0; SIG0(k0+1)=1;

%initial conditions for rho0 and sig0, fund solns to right of k0
rho0 = rho;
sig0 = sig;

% recusion loop for k>k0. Creates solutions to the right of k0.
for j = 2:((2*N+1)-k0)
   A=(1+alpha(j+k0-1)+alpha(j+k0-2))/alpha(j+k0-1);
   B = alpha(j+k0-2)/alpha(j+k0-1);
   rho0(j+1) = A*rho0(j) -B*rho0(j-1);
   sig0(j+1) = A*sig0(j) -B*sig0(j-1);
end

% recursion loop for k<k0. Creates solutions to the left of k0.
    for k = k0-1:-1:1
   A  = (1+alpha(k)+alpha(k+1))/alpha(k);
   B = alpha(k+1)/alpha(k);
   SIG0(k) = A*SIG0(k+1) -B*SIG0(k+2);
   RHO0(k) = A*RHO0(k+1) -B*RHO0(k+2);
    end
```

```
 sig0=sig0(3:length(sig0));
 %trims the repeat elements also in vector SIG0
 rho0=rho0(3:length(rho0));
 %trims the repeat elements also in vector RHO0

%the fundamental solns with initial starting point k0 are stored
% in row k0 of the matrix rhof and sigf
rhof(k0, :) =[RHO0 rho0];
sigf(k0, :) =[SIG0 sig0];
%%%%%%%%%%%%%%%%%%%%%%%%%%%%%%%%%%%%%%%%%%%%
%%%%%% this loop is for when k0=2*N+1. Had to create a separate loop
%%%%%% for this value of k0 in order to keep the length of row
%%%%%% k0=2N+1 uniform with the rest of the matrix.
    else
       RHO0(k0) = 1; RHO0(k0+1)=0;
       SIG0(k0) = 0; SIG0(k0+1)=1;
   %recursion loop for k<k0. When k0=2N+1 we only compute solns
   %to the left of k0.
   for k = k0-1:-1:1
   A  = (1+alpha(k)+alpha(k+1))/alpha(k);
   B = alpha(k+1)/alpha(k);
   SIG0(k) = A*SIG0(k+1) -B*SIG0(k+2);
   RHO0(k) = A*RHO0(k+1) -B*RHO0(k+2);
   end
   %These are the last two rows of the matrices rhof and sigf,
   %respectively.
    rhof(k0, :)= RHO0(1:2*N+1);
```

```
    sigf(k0, :)= SIG0(1:2*N+1);
    end
end
end
```

LIST OF REFERENCES

[1] D.G. Aronson, N.V. Mantzaris, and H.G. Othmer, *Wave propagation and blocking in inhomogeneous media,* Discrete Cont. Dynam. Systems, 13 (2005), pp. 843-876.

[2] J.W. Cahn, *Theory of crystal growth and interface motion in crystalline materials,* Acta Met 6 (1960) pp. 554-661.

[3] J.W. Cahn, J. Mallet-Paret, and E.S. Van Vleck, *Traveling wave solutions for systems of ODE's on a two-dimensional spatial lattice*, SIAM J. Appl. Math., 59(1998), pp. 455-493.

[4] C.E. Elmer and E.S. Van Vleck, *Spatially discrete FitzHugh-Nagumo equations*, SIAM J. Appl. Math., 65(2005), pp. 1153-1174.

[5] C.E. Elmer, *Finding stationary fronts for a discrete Nagumo and wave equation; construction*, Physica D. 218 (2006) pp.11-23.

[6] G. Fath, *Propagation failure of traveling waves in discrete bistable medium*, Phys. D, 116 (1998), pp. 176-190.

[7] A.R. Humphries, B.E. Moore and E.S. Van Vleck, *Fronts for bistable differential-difference equations with inhomogeneous diffusion*, SIAM J. Appld. Math. 71 (2011), pp. 1374-1400.

[8] T.J. Lewis and J.P. Keener, *Wave-block in excitable media due to regions of depressed excitability*, SIAM J. Appl. Math., 61 (2000), pp. 293-316.

[9] H.P McKean, Jr., *Nagumo's Equation*, Advances in Mathematics. 4 (1970), pp. 209-223.

[10] B.E. Moore and J.M. Segal, *Stationary bistable pulses in discrete inhomogeneous media*, Journal of Difference Equations and Applications 20.1 (2014), pp. 1-20.

[11] J. Sneyd and J. Sherratt, *On the propagation of calcium waves in an inhomogeneous media,* SIAM J. Appl. Math., 57 (1997), pp. 73-94.

[12] G. Teschl, *Jacobi Operators and Completely Integrable Nonlinear Lattices*, Math. Surveys Monogr. 72, American Mathematical Society, Providence, RI, 2000.